An Open Database to Evaluate the Fundamental Frequency of Historical Masonry Towers through Empirical and Physics-Based Formulations

Arnaud Montabert, Cédric Giry, Claire Limoge Schraen, Jade Lépine, Clarisse Choueiri, E. Diego Mercerat, Philippe Guéguen

buildings

MDPI

Article

An Open Database to Evaluate the Fundamental Frequency of Historical Masonry Towers through Empirical and Physics-Based Formulations

Arnaud Montabert [1,*,†], Cédric Giry [1,*,†], Claire Limoge Schraen [2], Jade Lépine [3], Clarisse Choueiri [3], E. Diego Mercerat [4] and Philippe Guéguen [5]

[1] Université Paris-Saclay, ENS Paris-Saclay, CentraleSupélec, CNRS, LMPS—Laboratoire de Mécanique Paris-Saclay, 91190 Gif-sur-Yvette, France
[2] Equilibre Structures, 10 Rue Saint Nicolas, 75012 Paris, France; c.schraen@unanimesentier.onmicrosoft.com
[3] Université Paris-Saclay, ENS Paris-Saclay, Department of Civil and Environmental Engineering, 91190 Gif-sur-Yvette, France; jade.lepine@ens-paris-saclay.fr (J.L.); clarisse.choueiri@ens-paris-saclay.fr (C.C.)
[4] Equipe REPSODY, CEREMA Méditerranée, 500 Route des Lucioles, 06903 Sophia Antipolis, France; diego.mercerat@cerema.fr
[5] ISTerre, Université Grenoble Alpes, CNRS, IRD, Université Savoie Mont-Blanc, Université Gustave Eiffel, 38058 Grenoble, France; philippe.gueguen@univ-grenoble-alpes.fr
* Correspondence: arnaud.montabert@ens-paris-saclay.fr (A.M.); cedric.giry@ens-paris-saclay.fr (C.G.)
† These authors contributed equally to this work.

Abstract: The fundamental frequency plays a primary role in the dynamic assessment of Cultural Heritage towers. Local and global features may impact its value: geometric, material features, interaction with the soil and adjacent buildings, aging, the construction phase, and repairs. A database is assembled to study the relationship between the fundamental frequency and the slender masonry structure features. Empirical and physics-based approaches were developed to assess the fundamental frequency from different sources of information. A Rayleigh–Ritz approach is proposed and compared with a 3D finite element model. A sensitivity analysis is then performed to quantify the contribution of each feature. As expected, it is shown that the height of the tower contributes the most to the fundamental frequency. The other tower features have a second-order impact on both the fundamental frequency and the mode shape. A comparison between the different approaches shows that the Rayleigh–Ritz drastically minimizes the difference between numerical and experimental frequencies when all information is available. Empirical relations are a good compromise when less information is available.

Keywords: slender structures; historical structures; masonry; operational modal analysis; Rayleigh–Ritz; database; sensitivity analysis

Citation: Montabert, A.; Giry, C.; Limoge Schraen, C.; Lépine, J.; Choueiri, C.; Mercerat, E.D.; Guéguen, P. An Open Database to Evaluate the Fundamental Frequency of Historical Masonry Towers through Empirical and Physics-Based Formulations. *Buildings* **2023**, *13*, 2168. https://doi.org/10.3390/buildings13092168

Academic Editor: Bartolomeo Pantò

Received: 25 July 2023
Revised: 19 August 2023
Accepted: 22 August 2023
Published: 26 August 2023

1. Introduction

Masonry towers belong to a peculiar structural typology in Cultural Heritage buildings. They are mainly diffused in the form of defensive towers, bell towers, clock towers, watch towers, etc., and can be found in every place in the world. Because they bear witness to a history spanning several centuries, they are a capital of irreplaceable cultural, social, environmental, and economic values. However, science can play a fundamental role in increasing and disseminating knowledge about heritage towers' history, composition, and behavior. This work is an opportunity to share with the community a database of historic slender heritage structures, as well as tools to help protect them, following on from previous pioneering works, e.g., [1–3].

The historical structures were mainly designed to withstand only vertical loads. They are, however, particularly vulnerable to seismic activity. The last Italian earthquakes in

L'Aquila (April 2009), Emilia-Romagna (May 2012), and Amatrice (August 2016), highlighted the high seismic vulnerability of the specific typology of slender masonry structures. The weak mechanical properties, the geometric features of the structure, and the soil–structure interaction generally explain this vulnerability.

Since the first mode of slender structures generally exhibits the highest mass participation, the value of the fundamental frequency plays a prominent role in assessing its dynamic behavior [4]. Its evaluation is suggested in some codes and provisions, such as the Italian guidelines for the assessment and mitigation of the seismic risk to cultural heritage [5], where their dynamic behavior is roughly comparable to either a cantilever equivalent beam or those that can be obtained from trustworthy simplified formulations.

On the other hand, modal parameters may be extracted from vibration measurements through operational modal analysis (see [6] for a review). This non-invasive dynamic identification is particularly suitable for Cultural Heritage structures. In the last decade, databases of the dynamic properties, materials, and geometric features of slender masonry structures have been assembled [1–3,7]. It has opened new opportunities to challenge the classical simple formulations and to design empirical formulations to estimate the fundamental frequency of slender masonry towers. The contribution of other parameters like the interaction with adjacent buildings [8] and the openings have been evaluated [2]. Despite considering many global features, we note the persistent variability of the fundamental frequency, which prompts us to consider more local features. Cultural heritage buildings may be strongly affected by the construction history, aging, repairs, retrofitting actions, bell systems, etc., e.g., [9].

In this work, we propose to quantify the contribution of global and local features when evaluating the fundamental frequency of slender masonry towers. The first step aims to gather existing databases [1–3,7], extended by a survey performed by the authors and isolated studies identified from an exhaustive literature review. Additional features have been added, such as the construction periods, local geometric features (thickness, openings geometry), and details about the measured fundamental frequency, the setup of the vibration analysis survey, and the technique used to identify modal parameters. The Towers featURes & fRequencIes databaSe (TURRIS) database is first described. Descriptive statistics provide information on the parameters well constrained by the data, which is necessary to study their impact on the fundamental frequency using the models proposed in the following section. Instrumentation practices and the extraction of modal characteristics also make it possible to discuss potential sources of uncertainty in fundamental frequency identification. We update empirical and physics-based models derived from existing relations found in the literature [1,10–15] to consider the tower dynamic features. The regression coefficients of the empirical formulations are updated. Empirical and physics-based models are then tested and discussed in light of the collected database. Additional parameters, such as the interaction with the soil, adjacent buildings, and the bells system, are then used in the Euler–Bernoulli beam formulation to test their impact on the dynamic properties. A semi-analytical Rayleigh–Ritz approach is then introduced to evaluate the dynamic properties of slender masonry structures. The formulation is calibrated through a comparison with a 3D finite element model. The results of evaluating the fundamental frequencies using empirical, physics-based, and Rayleigh–Ritz approaches are discussed. A sensitivity analysis based on the Random Balance Design Fourier-Amplitude Sensitivity Test (RBD-FAST) is used to test the sensitivity of the fundamental frequency to the structural features when using the Rayleigh–Ritz approach. The limits of the values of the parameters tested are taken from the descriptive statistical analysis of the database. It allows us to discuss future experimental efforts required to constrain the evaluation of the fundamental frequency. A significant result of this work is sharing a database and codes for evaluating the fundamental frequency of slender structures using empirical, physics-based models and Rayleigh–Ritz formulation. Both are available at the following GitHub link: https://github.com/MArnaud/TURRIS [16].

2. Masonry Towers Database

2.1. Parameters Describing the Towers

In the TURRIS database, the towers are described in terms of the associated literature reference; tower location (town, geographic coordinates); tower name; modal, geometric, and material parameters; construction period; details about the instrumental survey; and type of modal parameter identification technique. Modal parameters consist of the measured natural frequencies and the nature of the mode shape described in each reviewed paper. The geometry of each tower is simply described from its total and effective height (i.e., the height of the portion of the tower that is free from the restraint offered by adjacent buildings); the dimension of the ground section (length, width); the minimum and maximum thickness of walls; dimensions of openings (altitude, height, and width); its relation with adjacent buildings (isolated or bounded); and the mass of bells. Material parameters are described with the density, Young modulus, and Poisson's ratio. When available, the year or the century of construction is specified. The instrumental surveys are detailed with the type of instruments, the campaign duration, and the sampling of records.

2.2. Compilation of Data Collection

The data is assembled through an extensive literature review, including previously compiled data collections, isolated studies, and the authors' recent measurements (references, e.g., [1–3,7,8,12,13,17–181]). Values from previous data collection have been cross-checked, and additional information from the original papers has been included. Figure 1 highlights the number of instrumented slender masonry structures through time. The first instrumentation of a masonry tower was performed in 1989 [24]. We note some remarkable data collection. In 1995, Lund et al. [7] reported the vibration results of 19 old masonry towers in the Northeast of England to investigate the impact of the English bells system on the bell towers' behaviors (LU collection). In 2007 and 2009, Schmidt [17,18] presented experimental investigations of 16 twin bell towers in Saxony-Anhalt (Germany) and investigated the relationship between the natural frequencies and the geometric parameters of the towers (SC collection). In 2011, Rainieri and Fabbrocino [19] conducted an output-only modal identification of nine masonry towers (RF collection) in the Molise Region (Southern Italy) and compared the measured fundamental frequencies with the empirical relation provided by the Italian Seismic Code (NTC2008, [182]). In 2016, Limoge [20] reported an extensive dynamic identification survey of 20 baroque churches in French Savoy (France) to conduct a large-scale vibration-based model updating process (LI collection). In 2017, the Ziegler consultant group [21] published a report for the dynamic assessment of 18 masonry towers in Switzerland (Z collection). In 2020, Ruiz-Jaramillo et al. [22] conducted a large-scale survey of 21 watchtowers along the Southeast Spanish coast, providing valuable data for low-rise masonry towers (RJ collection). As part of the ACROSS ANR project, Mercerat et al. [23] identify the modal parameters of six medieval bell towers in the Mugello area (Tuscany, Italy). Some of the collections have been used in the compiled database proposed by Shakya et al. [1], Bartoli et al. [8], and Pallarès et al. [3].

Before 2011, dynamic identification is mainly performed to investigate the structural response of old towers under service loads, such as bell loads (e.g., [7]). However, the Italian earthquakes (L'Aquila and Amatrice) have led to increasing attention to the seismic behavior of historical structures, inducing an increase in dynamic identification studies.

Figure 2 shows the location of the 244 instrumented Cultural Heritage towers. Italy contributes most extensively to the collection of instrumented towers (44% of instrumented towers), resulting from a dense slender heritage, one of Europe's most significant seismic activities, and a preservation policy since the last damaging Italian earthquakes.

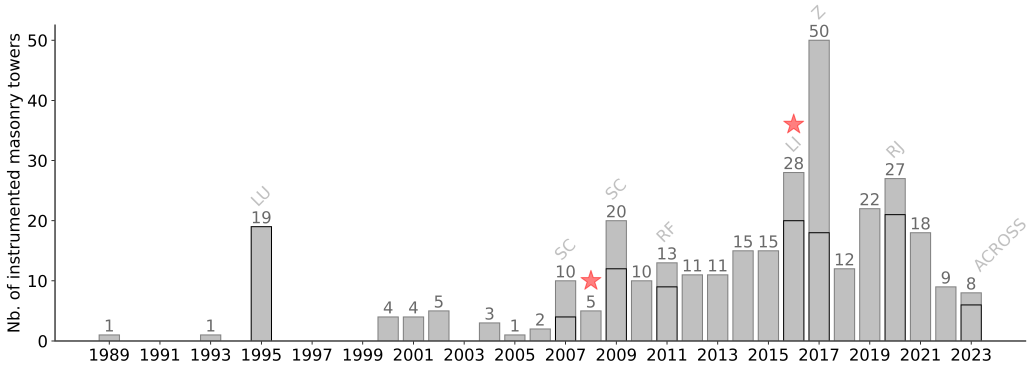

Figure 1. Graph of publication year for dynamic identification of slender Cultural Heritage towers in the compiled database for this study. The main previous database collections are indicated with black edge bar: LU [7], SC [17,18], RF [19], LI [20], Z [21], RJ [22], ACROSS [23]. The 2008 L'Aquila and 2016 Amatrice seismic events are reported with a red star.

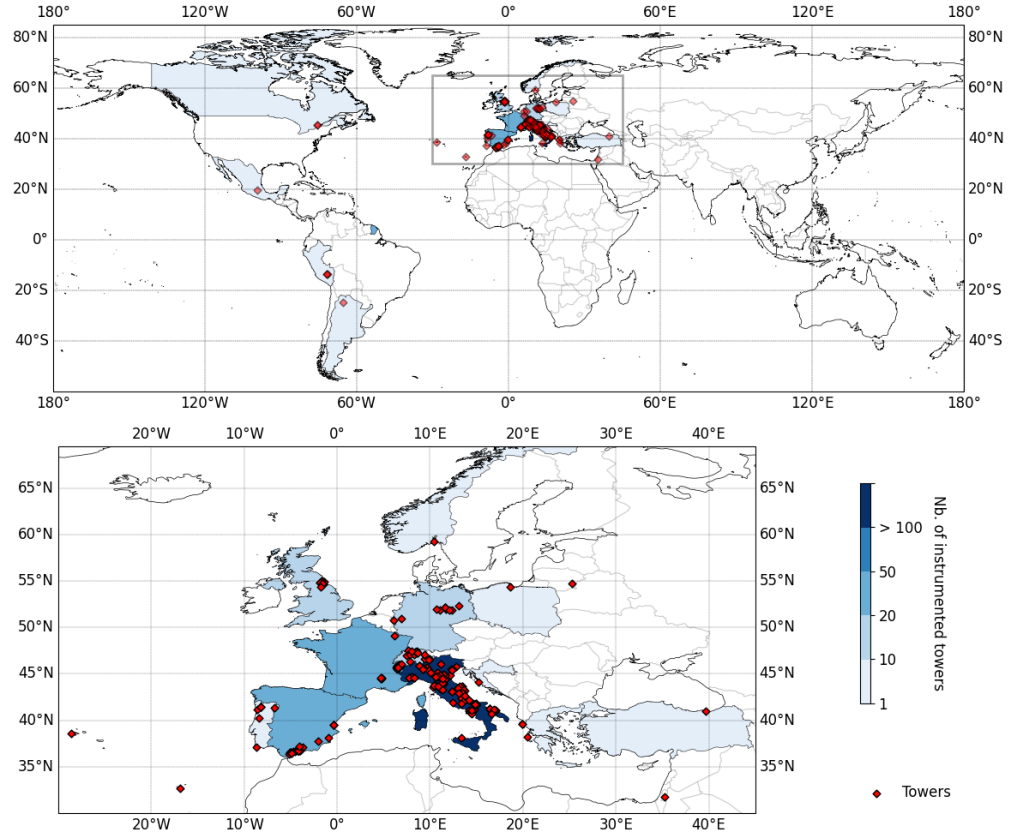

Figure 2. Locations of instrumented slender Cultural Heritage towers in the database.

2.3. Statistical Description

Figure 3 depicts the distribution of six geometric parameters of the database: the height H, the effective height H_{eff} (defined by [8] as the difference between the absolute height of the tower and the height of its constrained portion), the length L_s, the width ℓ_s, and the minimum and maximum thickness of walls t_w. The dimensions were reported from the articles' descriptions or plans when available. When both pieces of information are available, an error in the order of a decimeter is generally observed, which can impact the dynamic properties and then motivate a sensitivity analysis in the rest of the study.

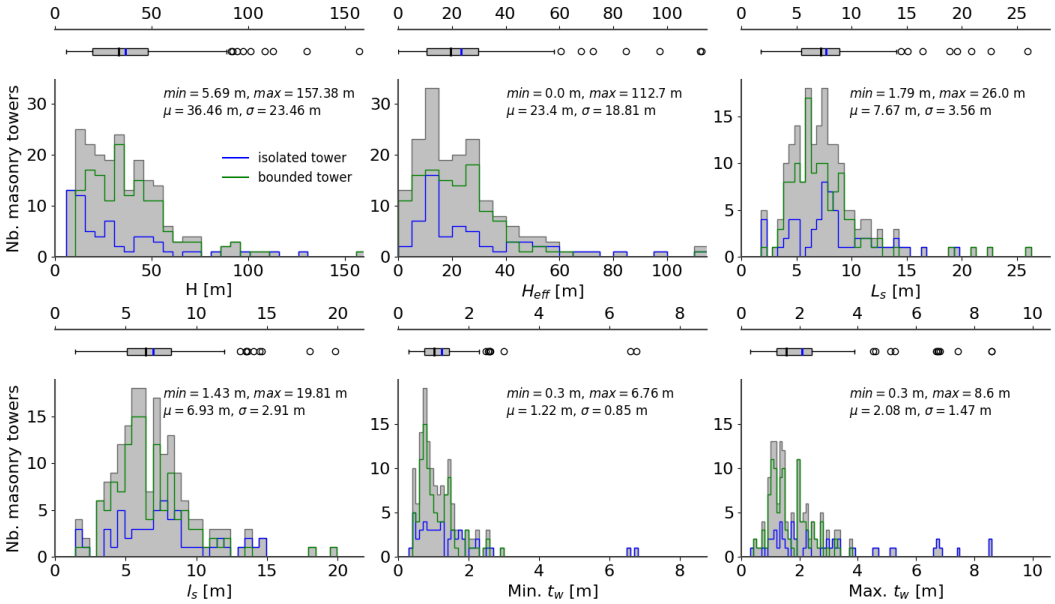

Figure 3. Distribution of the geometric parameters of the Cultural Heritage towers assembled in the database: the height H, the effective height H_{eff}, the length L_s, the width ℓ_s, the minimum and maximum thickness of walls t_w. The median and mean values are shown in black and blue, respectively. The distribution of isolated towers is shown in blue. The distribution of the bounded towers is shown in green.

The six parameters highlight a right-skewed bimodal distribution. The bimodal distribution can be explained when distinguishing between isolated and bounded towers. We generally observe small and wide isolated towers but large and narrow linked towers.

The distribution asymmetry reveals only a few historical masonry towers with large dimensions (therefore, insufficient sampling for towers with important geometric characteristics). Indeed, most of the towers (75%) have a height between 5.69 m (water tower number 3 in Pompeii, in [134]) and 48.0 m, an effective height lower than 29.97 m (the database contains 65 isolated towers and 177 bounded towers), a length between 1.79 m and 8.75 m, a width between 1.43 m and 8.2 m, and a wall thickness between 0.3 m and 2.5 m. We note the presence of a few outliers for each parameter. The highest tower (157.38 m) corresponds to the Northern tower of the Cologne cathedral, known as the tallest twin-spired church in the world. The tower of the Universidad Laboral (130.0 m), the Torrazzo di Cremona (112.70 m), the Guglia Maggiore tower of the Duomo (108.50 m), and the twin bell towers of the cathedral in Magdeburg (101.0 m) are among the tallest instrumented towers of this study, and are not representative of the standard dimension of ancient masonry towers. The towers mentioned above also classify as outliers when considering the effective height.

Some remarkable Cultural buildings such as the Tower of Pisa (Italy), the Giotto's bell tower (Italy), the North Tower of the Cologne Cathedral (Germany), the Guglia Maggiore Tower of the Duomo (Italy), the twin bell towers of the Cathedral in Halberstadt (Germany), the Calbe Stephani church (Germany), the Moya tower (Spain), and the Umong pagoda (China) highlight huge section (length and width). The outliers for the wall thickness are mainly composed of the watchtowers along the Spanish coast, since many are filled towers.

Figure 4 shows the material parameter distributions of the masonry towers when available. Most values come from building codes or model updating processes, minimizing the difference between the measured and numerical modal parameters. These values are then indirectly identified. Such an origin should be kept in mind in the rest of the study. Only 42.4% of the reviewed studies provide a value for the Young modulus, 12.5% for the Poisson ratio, and 28% for the density. The Young modulus highlights a right-skewed bimodal distribution. The highest Young modulus values are related to retrofitting actions using concrete that have been considered in the model updating process. They may induce

a bias in the distribution, since they are not masonry. The two modes are observed around 1.52 GPa and 3.96 GPa. Despite the limited number of values, the Poisson ratio and the density have a more symmetric distribution. It is important to note that most studies impose the value of the Poisson ratio.

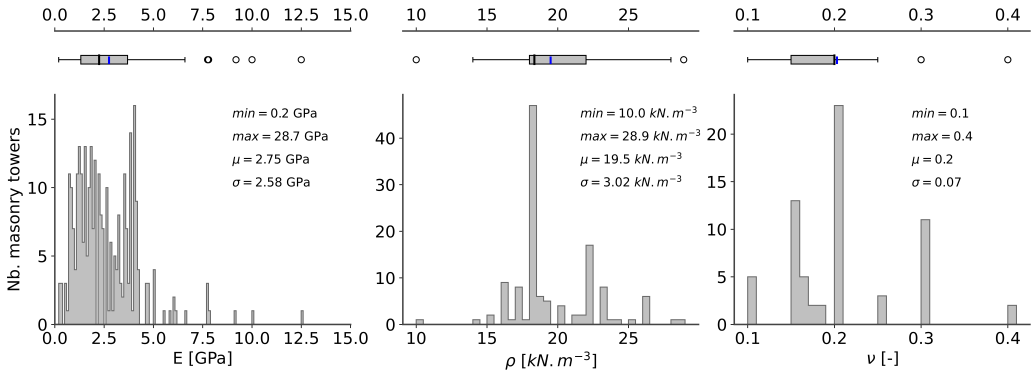

Figure 4. Distribution of material parameters of the masonry towers database. The median and mean values are shown in black and blue, respectively.

When the values are available, the mass of the bells is reported in the database. It constitutes an essential mass on top that can impact the modal behavior of the slender structures. The bells are usually located at the top of the tower. Figure 5 again shows an asymmetric distribution of the bell's mass. Among the outliers (over 10,000 kg), there are the church of Nuestra Señora Candelaria de la Viã (Argentina), as well as three bell towers of the French Savoy (LI collection).

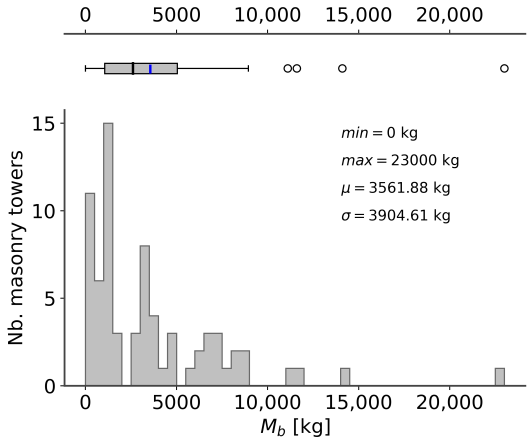

Figure 5. Distribution of bell mass of the masonry towers database. The median and mean values are shown in black and blue, respectively.

Figure 6 shows that most of the instrumented towers were built in the medieval period, which induced a potential vulnerability of the structures studied due to the decay of the mechanical properties (mortar and bricks). We note a second group of structures built between the 19th and 20th centuries. The oldest masonry towers are Pompeii's water towers, which date from the 1st century BC.

Figure 7 shows the distribution of the recording times during the OMA survey. Short and long SHM are, respectively, plotted on left and right (long SHM concern surveys lasted more than one day). Most of the studies (83%) consist of a short SHM. The white noise hypothesis in OMA is still debated and may impact dynamic identification. Rodriguez et al. [183] and Cantieni [184] recommended the measurement duration to be at least 2000 times the natural period of interest in the case of slender masonry structures in order to reduce uncertainties. Studies respecting this empirical law are shown in green in Figure 7.

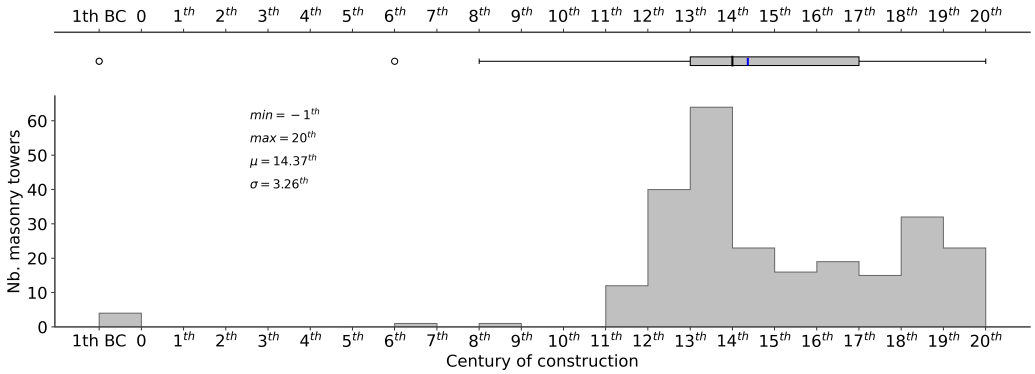

Figure 6. Distribution of the century of bell tower construction. The median and mean values are shown in black and blue, respectively.

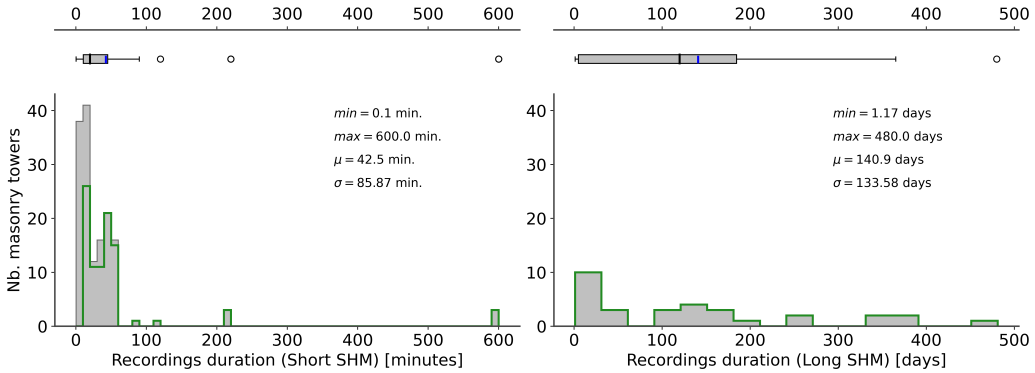

Figure 7. Distribution recordings duration during OMA surveys. The median and mean values are shown in black and blue, respectively. Instrumentations respecting a measurement duration longer than 2000 times the natural period of interest established by Rodriguez et al. [183] and Cantieni [184] are shown in green.

Many OMA techniques have been developed in recent decades (Table 1) due to their many advantages: they are a non-invasive, non-destructive method, easy to deploy, and no external source is required. The output-only method is particularly adapted in the context of Cultural Heritage Monitoring since it allows model parameter tracking in a non-invasive way. However, these techniques have different precision to identify natural frequencies. Figure 8 shows the use of the OMA techniques in the dynamic identification of slender masonry structures. Generally, they can be classified into two categories: frequency domain and time domain (in gray and blue, respectively, in Figure 8). Frequency domain techniques have been largely used in masonry towers (69.1%) compared to time domain techniques. The earliest methods are based on a peak-picking algorithm from diverse frequency representations of the record: the power spectral density (PSD), the fast Fourier transform (FFT), the acceleration spectral amplitude (ASA) or displacement (ASD), and the transfer function (TF). The natural frequency is then directly obtained from the choice of the peak. Despite its simplicity, the technique suffers from difficulty in distinguishing close modes, and its limitation of the spectrum frequency resolution contributes to an increase in the uncertainty of the natural frequency identification [185,186]. Peak picking from frequency graphs represents 3% of the data in the masonry tower database. Consequently, the frequency domain decomposition (FDD) was developed to meet the challenge when identifying close modes [187], and is used in 12.5% of the instrumented towers. The structure's response is derived into a set of single-degree-of-freedom systems by introducing a decomposition of the spectral density function matrix. The enhanced FDD (EFDD) has also been introduced to extract the damping ratios, representing 14.23% of the case studies. However, these frequency domain methods are under the assumption that the input signals are stationary Gaussian white noise, and the structure is very lightly damped. At

the same time, methods in the time domain have been developed. Techniques from the experimental modal analysis, such as Random Decrement Technique (RDT) and eigen realization algorithm (ERA), were also successfully extended for the OMA, but have rarely been applied to the dynamic identification of slender masonry towers (one case for the ERA method, and two cases for the RDT technique). Furthermore, much research was spent on subspace identification techniques [188], which constitute 21.5% of the measured frequencies in the masonry towers database. The two primary forms of Stochastic Subspace Identification (SSI) techniques used in the database are Covariance-Driven Stochastic Subspace Identification (COV-SSI) and Data-Driven Stochastic Subspace Identification (DATA-SSI), in 10% and 3%, respectively. A total of 46% of studies using SSI techniques do not specify which method is used (they only mention SSI).

Table 1. Acronyms of methods used to extract modal parameters described in this section.

Glossary	
TFIE	Time Frequency Instantaneous Estimators
PRTD	Polyreference time domain
DSPI	Direct system parameter identification
SSI	Stochastic Subspace Identification
CC-SSI	Crystal Clear Stochastic Subspace Identification method
SSI-COV-PC	Principal Component Covariance-Driven Stochastic Subspace Identification
SSI-DATA	Data-Driven Stochastic Subspace Identification
SSI-DATA-UPC	Unweighted Principal Component Stochastic Subspace Identification
SSI-DATA-CVA	Canonical Variate Analysis
ASA	Acceleration Spectral Amplitudes
ASD	Auto-Spectrum Displacement
ERA	Eigensystem realization algorithm
SM	stretching method
TF	Transfer function
SOBI	Second Order Blind Identification
PSD	Power Spectral Density
SSR	Standard Spectral Ratio
SDOF	Single Degree of Freedom technique
p-LSCF	Poly-reference Least Squares Complex Frequency-domain

Figure 9 shows the distribution of the experimental fundamental frequency variation for each instrumented masonry tower. Masonry towers for which there is only a single value of the fundamental frequency are excluded from the figure, as they do not provide any information about the variations in the dynamic properties of the structure studied (83% of the studies). Most of the main frequency variation is between 0.13% and 32.39% (the San Luzi bell tower) and has several origins. Considerable variations in the fundamental frequency are observed before and after restoration works. The SS. Annunziata church bell tower, significantly damaged by an earthquake, shows a fundamental frequency of 1.66 Hz [127] and 1.97 Hz after restoration [32], an increase of 18.7%. In 2005, the Mogadouro Clock Tower was characterized by large cracks, deterioration, and material loss in some parts. Following restoration work in 2005, the fundamental frequency was raised from 2.15 to 2.56 Hz (an increase of 19%). The same phenomenon is observed in the tower of the S. Giorgio church in Trignano. Following the 1996 Reggio Emilia earthquake, restoration works led to the main frequency from 2.43 Hz to 2.7 Hz (an increase of 11% on the fundamental frequency). The bell tower of Sant Andrea Apostolo highlights an increase in its fundamental frequency of 27.08% after retrofitting actions [102,103]. The tower of Notre Dame de l'Assomption, damaged after Le Teil earthquake, highlights a double fundamental frequency peak (Mercerat, personal communication). Structure monitoring over long periods shows significant variations. Monitoring of the San Luzi bell tower over a whole year shows a variation of 32.29% between winter and summer [87]. The bell tower of the church of San Frediano highlights a variation of 14% due to the impact of environmental parameters [67].

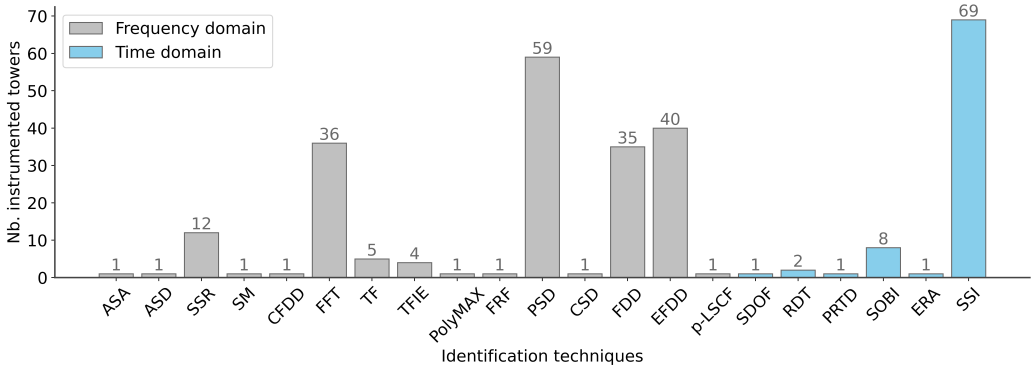

Figure 8. Distribution of the identification techniques used in the database. Abbreviations are summarized in the glossary (Table 1).

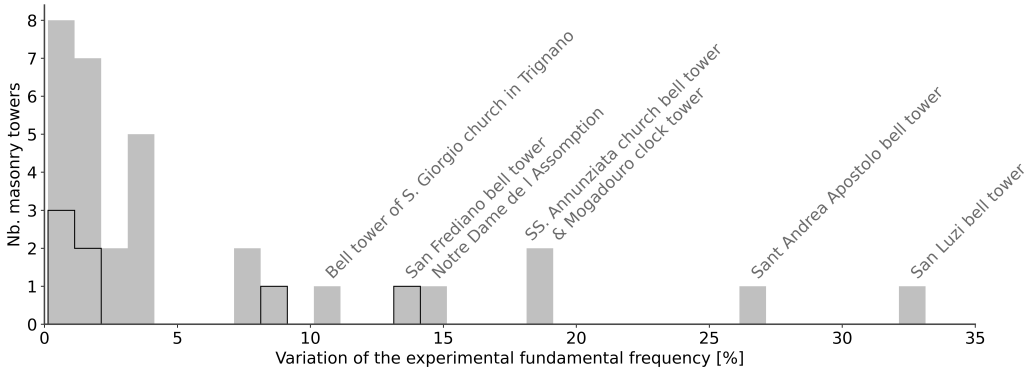

Figure 9. Distribution of variation in the measured fundamental frequency expressed as $(f_0^{max} - f_0^{min})/f_0^{min}$, i.e., the maximum difference between the minimum and maximum measured fundamental frequency for each instrumented masonry tower. Long SHM (with measurements duration over one day) are plotted with a dark gray edge.

3. Model for the Evaluation of the Fundamental Frequency of the Tower

3.1. Empirical Models

The models exposed here propose to estimate the fundamental frequency of slender masonry structures according to the global geometric parameters expressed in Table 2. To analyze these models, let us define a set of global geometric parameters $\boldsymbol{p}$ that characterize the structures: $\boldsymbol{p} = \{H, \ell_s, h_n\}$. The height of interaction h_n between the tower and any adjacent structures is expressed as $h_n = H - H_{eff}$. Dimensionless parameters are introduced: $\alpha_\ell = \ell_s / H$ and $\alpha_{h_n} = h_n / H$.

In the empirical model's category, we consider models that integrate the main parameters that influence the fundamental frequency of the structures without deriving their expression from mechanical models (e.g., a power law with an exponent identified from a regression process). We introduce the empirical model derived from the reference summarized in Table 3 as follows:

$$f_0(\boldsymbol{p}) = a_1 \cdot H^{b_1} \cdot f_s(\alpha_\ell) \cdot f_e(\alpha_{h_n}) \tag{1}$$

The function associated with the influence of the geometric characteristics of the section f_s is as follows:

$$f_s = (\alpha_\ell)^{b_1^s} \cdot \left(1 + a_1^s \alpha_\ell + a_2^s \alpha_\ell^2 + a_3^s \alpha_\ell^3\right)^{b_2^s} \tag{2}$$

The function associated with the interaction with adjacent structures f_e is as follows:

$$f_e = (1 - \alpha_{h_n})^{b_1^e} \tag{3}$$

Table 2. Set of geometric parameters and regression coefficients used in the empirical formulation of geometric models.

Nomenclature		
Symbol	**Unit**	**Description**
Geometric parameters		
$\boldsymbol{p}$		Set of global geometric parameters
H	[m]	Height of the tower
ℓ_s	[m]	Width, lowest size of the tower's section
h_n	[m]	Height of interaction between the tower and any adjacent structures system
f_0	[Hz]	Eigenfrequency
Dimensionless parameters		
α_ℓ	[-]	Slenderness
α_{h_n}	[-]	Interaction factor
Regression coefficients		
b_1	[-]	Regression coefficient related to the height
a_1^s, b_1^s, b_2^s, a_2^s, a_3^s	[-]	Regression coefficient related to the section geometry
b_1^e	[-]	Regression coefficient related to lateral interaction

Table 3. Parameters of existing and updated empirical models. Line labeled from Empirical model 1 to 7 correspond to this study.

Id. Model	**Ref.**	a_1	b_1	a_1^s	b_1^s	b_2^s	a_2^s	a_3^s	b_1^e
1	[10]	20	−3/4	0	0	0	0	0	0
1	[11]	1/0.0187	−1	0	0	0	0	0	0
1	[12]	1/0.01137	−1.138	0	0	0	0	0	0
1	[1]	1/0.0151	−1.08	0	0	0	0	0	0
1	[13] [b]	28.35	−0.83	0	0	0	0	0	0
1	[13] [i]	135.343	−1.32	0	0	0	0	0	0
Empirical model 1		22.55	2.818	0	0	0	0	0	0
2	[1]	3.58	0	0	0.57	0	0	0	0
Empirical model 2		7.608	0	0	0.817	0	0	0	0
3	[13] [i]	208.54	−1.18	0	0.55	0	0	0	0
Empirical model 3		17.113	−0.369	0.538	0	0	0	0	0
4	[14]	1/0.06	−0.5	2	0.5	0.5	0	0	0
4	[1]	1/0.03	−0.83	1	0.17	0.5	0	0	0
Empirical model 4		7.361	−0.46	−0.03	0	3053.821	0	0	0
5	[15]	1/0.0117	0	−9.632	3	−1	94.786	144.461	0
Empirical model 5		0.1	0	−26.78	188.47	29.40	−34.47	13.93	0
6	[13] [b]	12.96	−0.686	0	0	0	0	0	−0.686
Empirical model 6		23.322	−0.695	0	0	0	0	0	−0.028
7	[13] [b]	14.61	−0.811	0	−0.254	0	0	0	−0.341
Empirical model 7		17.619	−0.365	0.616	0	0	0	0	−0.171

[b] Bounded tower. [i] Isolated tower.

Table 3 lists the coefficient of Equation (1) obtained through regression in the dedicated studies. Empirical models may be separated into seven models based on the parameters used and the power of the monomials. Each model is updated based on the assembled database. The results of the seven regression models (labeled from Empirical model 1 to Empirical model 7 in Table 3) are shown in Figure 10 with their associated coefficient of determination. They range from 0.48 (Empirical model 1) to 0.67 (Empirical model 7). The best prediction is obtained for model 7, taking into account the height of interaction h_n. However, this model depicts a coefficient of determination very close to the empirical model 4 that considered only H and l_s.

3.2. Physics Based Models

The models exposed here propose to estimate the fundamental frequency of slender masonry structures according to global geometric parameters, geometric section, and mate-

rial characteristics. Table 4 summarizes the parameters considered in these models. The set of global parameters is defined as $\boldsymbol{p} = \{H, \ell_s, h_n, t_w, L_s, E, \rho\}$. Additional dimensionless parameter are introduced: $\alpha_t = \frac{t_w}{\ell_s}$ and $\alpha_L = \frac{L_s}{\ell_s}$.

Table 4. Set of geometric and material parameters and regression coefficients used for the physics-based approach.

Nomenclature		
Symbol	**Unit**	**Description**
Geometrical and material parameters		
$\boldsymbol{p}$		Set of global geometric parameters
H	[m]	Height of the tower
ℓ_s	[m]	Width, lowest size of the tower's section
h_n	[m]	Height of interaction between the tower and any adjacent structures
f_0	[Hz]	Fundamental frequency
L_s	[m]	Length, largest size of the tower's section
t_w	[m]	Wall thickness
h_b	[m]	Altitude of the bell system
S	[m^2]	Surface area
I_{G_x}, I_{G_y}	[m^4]	Second moment of area
r	[m]	Radius of inertia
E	[MPa]	Young modulus
ρ	[kg·m^{-3}]	Volumetric mass density
Dimensionless parameters		
α_ℓ	[-]	Slenderness
α_{h_n}	[-]	Interaction factor
α_t	[-]	Thickness factor
α_L	[-]	Length factor
α_{sh}, α^I_{sh}, α_ℓ,	[-]	Section factor
θ	[rad.]	Angle of bending direction with respect to x axis
Regression coefficients		
C_1, C_2, C_3	[-]	Regression coefficient

This second category of models originates from the dynamic characteristics of an equivalent beam model. For a cantilever Euler–Bernoulli beam with homogeneous geometric and material properties, the fundamental frequency is expressed as:

$$f_0 \sim \frac{1.875^2}{2\pi} \cdot \frac{r}{H^2} \cdot \sqrt{\frac{E}{\rho}} \tag{4}$$

Considering classical shapes for the hollow section of the slender structures (see Figure 11, and Table 5), a generic formula can be derived for the radius of inertia r.

$$I_{G_x} = \alpha^I_{sh} \cdot \ell_s^4 \cdot \left(\alpha_L - (1-2\alpha_t)^3 \cdot (\alpha_L - 2\alpha_t)\right) = \ell_s^4 \cdot \alpha_{I_x}\left(\alpha^I_{sh}, \alpha_L, \alpha_t\right) \tag{5}$$

$$I_{G_y} = \alpha^I_{sh} \cdot \ell_s^4 \cdot \left(\alpha_L^3 - (1-2\alpha_t) \cdot (\alpha_L - 2\alpha_t)^3\right) = \ell_s^4 \cdot \alpha_{I_y}\left(\alpha^I_{sh}, \alpha_L, \alpha_t\right) \tag{6}$$

$$S = 2 \cdot \alpha^S_{sh} \cdot \ell_s^2 \cdot \alpha_t \cdot (\alpha_L + 1 - 2\alpha_t) = \ell_s^2 \cdot \alpha_A\left(\alpha^I_{sh}, \alpha_L, \alpha_t\right) \tag{7}$$

Table 5. Surface and second moment of area for different classical hollow sections of masonry tower (square (SQ), rectangular (REC), and circular (CIR)).

Parameters	**SQ**	**REC**	**CIR**
α^S_{sh}	1	1	$\pi/4$
α^I_{sh}	1/12	1/12	$\pi/64$
α_ℓ	1	>1	1

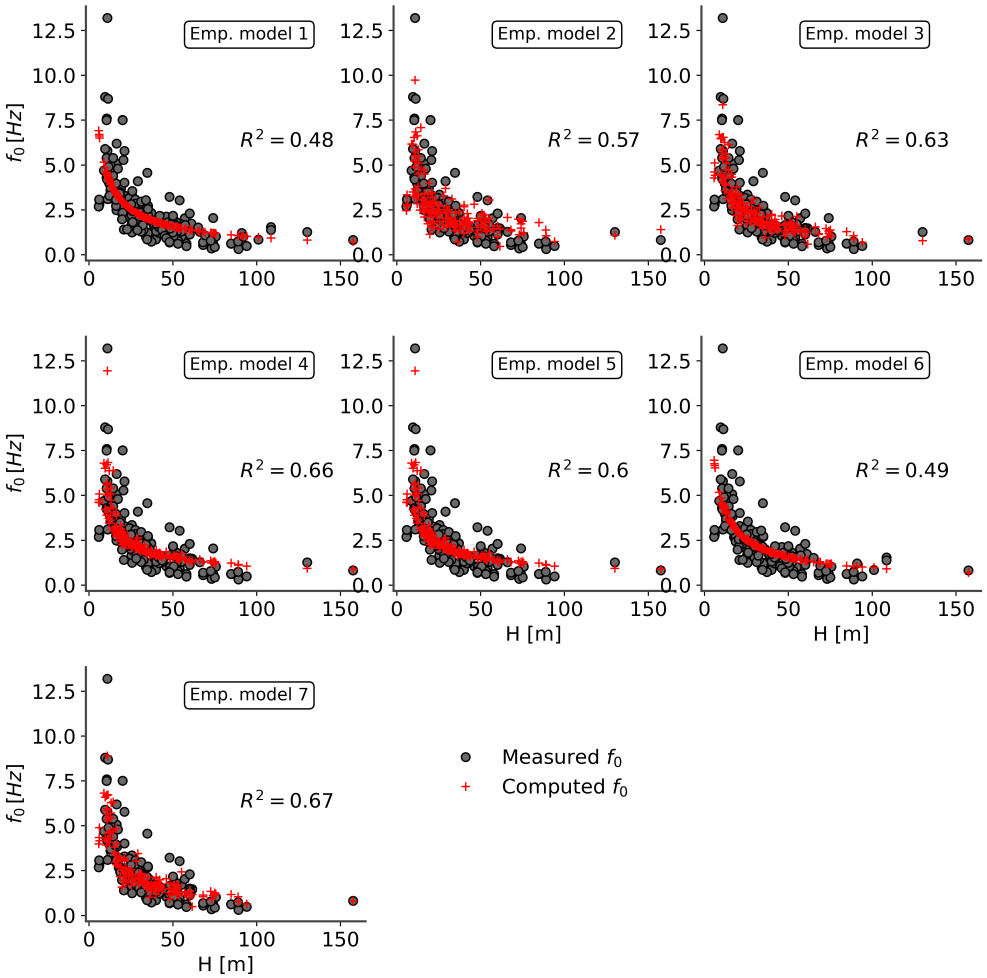

Figure 10. Evaluation of the fundamental frequency of towers from experimental natural frequency (gray dot) and empirical models (red cross) (labeled from Empirical model 1 to Empirical model 7 in Table 3) as a function of the tower's height.

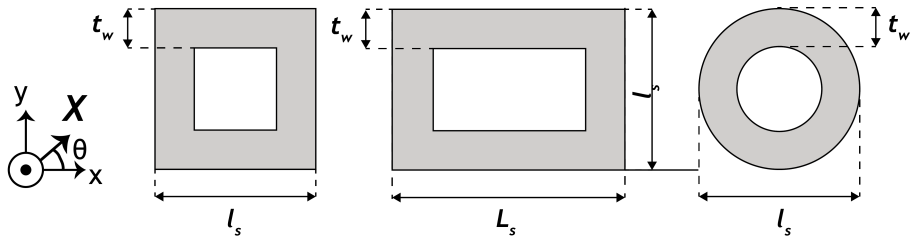

Figure 11. Parametric hollow sections: square (SQ), rectangular (REC), and circular (CIR).

The radius of inertia for simple hollow sections is

$$r_{G_X} = \ell_s \cdot \sqrt{\frac{1}{\alpha_A}} \cdot \sqrt{\frac{\alpha_{I_x} + \alpha_{I_y}}{2} + \frac{\alpha_{I_y} - \alpha_{I_y}}{2} \cdot \cos(2\theta)} \quad (8)$$

The models in this category are derived from the formula of the fundamental frequency of a cantilever beam with some simplification regarding the radius of inertia or the influence of the material characteristics. A generic formula for these models is expressed as:

$$f_0 = C_1 \cdot \frac{1.875^2}{2\pi} \cdot \frac{\tilde{r}}{H^2} \cdot \left(\frac{1}{1-\alpha_{h_n}}\right)^{C_2} \cdot \left(\sqrt{\frac{E}{\rho}}\right)^{C_3} \quad (9)$$

With the value of C_1, C_2, C_3, and $\tilde{r}$ summarised in Table 6.

Table 6. Parameters of the physics-based models.

Id Model	Ref.	C_1	C_2	C_3	$\tilde{r}$
1	[1]	$\sqrt{1.375}$	0	1	r_{G_X}
2	[8] (Equation (22))	0.8	1	1	$\frac{\ell_s}{\sqrt{12}} \cdot 1.5 \cdot (1-\alpha_t)$
3	[8] (Equation (23))	0.8	0	1	$\frac{\ell_s}{\sqrt{12}} \cdot 1.125$
4	[8] (Equation (24))	800	0	0	$\frac{\ell_s}{\sqrt{12}} \cdot 1.125$

The results of evaluating the fundamental frequency using physics-based relation are shown in Figure 12, restrained to the available data. It is important to note that the material properties used (and recorded in the database) are derived from calibrating finite element models based on vibration measurements. The second physics-based model shows the best prediction. The performance of these methods is inferior to that of the empirical formulation. One reason could be the incompatibility of material property values calibrated from more complex models.

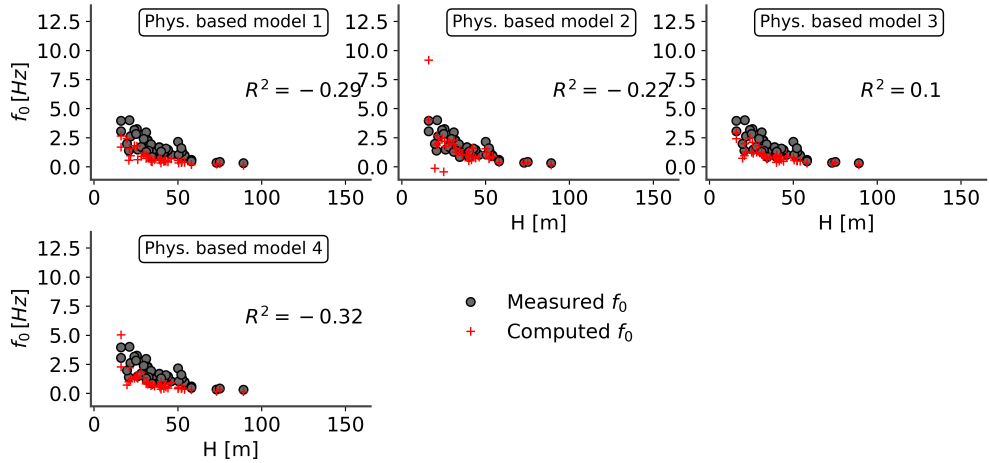

Figure 12. Evaluation of the fundamental frequency of towers from physics-based models (red cross) and experimental natural frequency (gray dot) as a function of the tower's height.

3.3. Description of the Timoshenko Beam

In this section, we propose introducing additional parameters to the physics-based models to consider the influence of the environment of the slender structures and the bell system (Table 7). The influence of the soil/structure interaction on the dynamic properties of the tower has been studied, for instance, in [189,190]. Furthermore, this model is used later to evaluate these properties' sensitivity to interactions parameters (soil/tower interaction, nave/tower interaction) and bell system. The model illustrated in Figure 13 is limited to describing flexural bending modes. All parameters are summarized in Table 7.

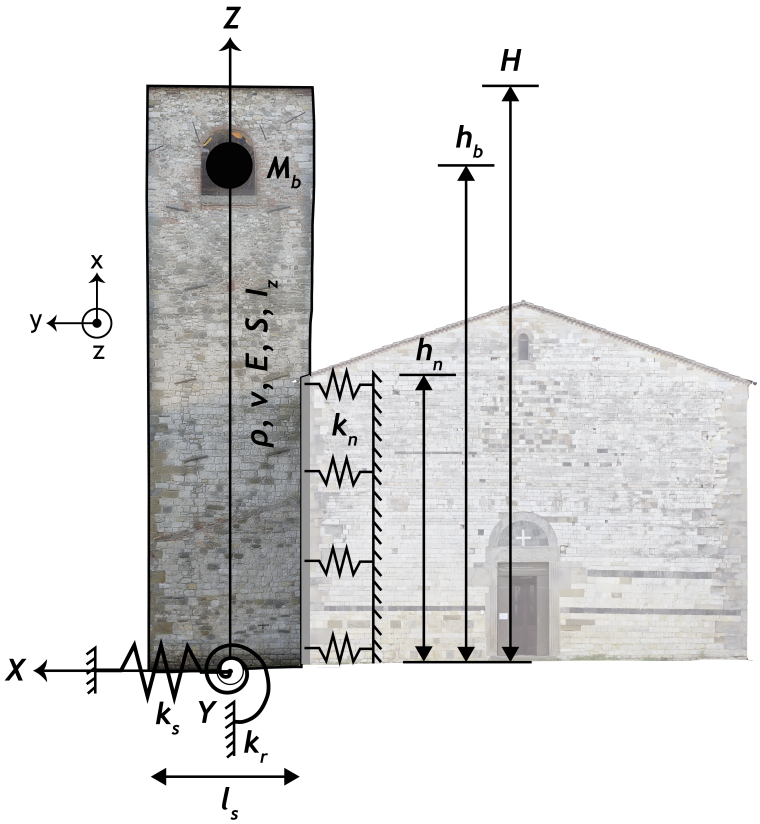

Figure 13. Model of the bell tower (Euler–Bernoulli beam model).

Table 7. Parameters and symbols used to describe the Rayleigh–Ritz approach.

Nomenclature		
Symbol	**Unit**	**Description**
$\boldsymbol{p}$		Set of global geometric parameters
H	[m]	Height of the tower
ℓ_s	[m]	Width, lowest size of the tower's section
h_n	[m]	Height of interaction between the tower and any adjacent structures
f_0	[Hz]	Eigenfrequency
L_s	[m]	Length, largest size of the tower's section
t_w	[m]	Wall thickness
h_b	[m]	Altitude of the bell system
S	[m^2]	Surface area
E	[MPa]	Young modulus
ρ	[$kg \cdot m^{-3}$]	Volumetric mass density
ν	[-]	Poisson ratio
I_z	[m^4]	Second moment of inertia
k_s	[$N \cdot m^{-1}$]	Soil/structure translational stiffness
k_r	[N]	Soil/structure rotational stiffness
k_n	[$N \cdot m^2$]	Nave/structure translational stiffness
M_b	[kg]	Mass of the bell system
G	[Pa]	Shear modulus
k	[-]	Shear coefficient
$v(x,t)$	[m]	Transversal deflection
$\theta(x,t)$	[rad.]	Normal rotation
$\mathcal{V}$	[J]	Potential energy
$\mathcal{T}$	[J]	Kinetic energy
$\mathcal{V}_{beam}$	[J]	Potential energy associated with the beam system
$\mathcal{V}_{SSI}$	[J]	Potential energy associated with the soil–structure interaction
$\mathcal{V}_{TNI}$	[J]	Potential energy associated with the tower-nave interaction system
$\mathcal{T}_{beam}$	[J]	Kinetic energy associated with the beam system
$\boldsymbol{\varphi}(x), \boldsymbol{\vartheta}(x)$	[-]	Polynomial functions to approximate the displacement and rotation field
$\boldsymbol{q}$	[-]	Generalized coordinates system
$\boldsymbol{M}, \boldsymbol{K}$		Mass and Stiffness matrix

The dynamic response of the tower alone is described by a Timoshenko beam model. Indeed, as it has been observed in [191], the Euler–Bernoulli beam model tends to overestimate the eigenfrequency of non-slender structures.

The structural parameters $\boldsymbol{p}$ for the tower of height H are

$$\boldsymbol{p} = \{H, S, I_y, k, E, \nu, \rho, k_s, k_r, k_n, h_n, M_b, h_b\} \tag{10}$$

3.4. Rayleigh–Ritz Method

The Rayleigh–Ritz method has been successfully used to approximate the dynamic characteristics of the Euler–Bernoulli (EB) beam (e.g., [192]) or Timoshenko (TIMO) beam (e.g., [28]) with additional masses or springs.

The potential energy $\mathcal{V}$ and the kinetic energy $\mathcal{T}$ for the model described in Figure 13 are: $\mathcal{V} = \mathcal{V}_{beam} + \mathcal{V}_{SSI} + \mathcal{V}_{TNI}$, $\mathcal{T} = \mathcal{T}_{beam} + \mathcal{T}_{bell}$. The energies associated with the beam $\mathcal{V}_{beam}$ and $\mathcal{T}_{beam}$ are

$$\mathcal{V}_{beam} = \frac{1}{2}\int_0^H \left\{ EI_z \left(\frac{\partial \theta}{\partial x}\right)^2 + kGS\left(\theta - \frac{\partial v}{\partial x}\right)^2 \right\} \mathrm{d}x \tag{11}$$

$$\mathcal{T}_{beam} = \frac{1}{2}\int_0^H \left\{ \rho S \left(\frac{\partial v}{\partial t}\right)^2 + \rho I_z \left(\frac{\partial \theta}{\partial t}\right)^2 \right\} \mathrm{d}x \tag{12}$$

where $v(x,t)$ is the transversal deflection and $\theta(x,t)$ is the normal rotation. For the sake of simplicity, the shear coefficient is estimated with the formulas for thin-walled structures in [193].

The energy for the soil–structure interaction $\mathcal{V}_{SSI}$ is

$$\mathcal{V}_{SSI} = \frac{1}{2}\left(k_r \left(\left.\frac{\partial v}{\partial x}\right|_0 \right)^2 + k_s (v|_0)^2 \right) \tag{13}$$

The energy for the tower-nave interaction $\mathcal{V}_{TNI}$ is

$$\mathcal{V}_{TNI} = \frac{1}{2}\int_0^{h_n} k_n v^2 \mathrm{d}x \tag{14}$$

The energy for the bell system $\mathcal{V}_{bell}$ is

$$\mathcal{T}_{bell} = \frac{1}{2} M_b \left(\left.\frac{\partial v}{\partial t}\right|_{h_b} \right)^2 \tag{15}$$

The displacement v and the rotation θ fields of the beam are approximated over simple polynomial functions $\boldsymbol{\varphi}(x)$ and $\boldsymbol{\vartheta}(x)$, and their coordinates in the polynomial basis $\boldsymbol{R(t)}$, and $\boldsymbol{V(t)}$,

$$v(x,t) \approx \sum_{i=0}^{n_H} V_i(t)\varphi_i(x), \quad \theta(x,t) \approx \sum_{i=0}^{n_r} R_i(t)\vartheta_i(x) \tag{16}$$

For the sake of simplicity, admissible functions (functions satisfying all the geometric boundary conditions) [194] are considered as the basis. For the cantilever beam, the following functions are used [195]:

$$\varphi_i(x) = \left(\frac{x}{H}\right)^2 \cdot \left(1 - \frac{x}{H}\right)^{i-1}, \quad \vartheta_i(x) = \left(\frac{x}{H}\right) \cdot \left(1 - \frac{x}{H}\right)^{i-1} \tag{17}$$

In the presence of soil–structure interaction, the functions corresponding to free–free boundary conditions are considered [195],

$$\varphi_i(x) = \left(1 - \frac{x}{H}\right)^{i-1}, \quad \vartheta_i(x) = \left(1 - \frac{x}{H}\right)^{i-1} \tag{18}$$

The size of the system for the Rayleigh–Ritz model is equal to $n_H + n_r$.

By considering $\boldsymbol{q}(\boldsymbol{V}, \boldsymbol{R})$ as a generalized coordinates system, the equation of Lagrange is

$$\frac{\mathrm{d}}{\mathrm{d}}\left(\frac{\partial \mathcal{T}}{\partial \dot{\boldsymbol{q}}}\right) + \left(\frac{\partial \mathcal{V}}{\partial \boldsymbol{q}}\right) = \boldsymbol{0} \tag{19}$$

After some mathematical developments, the equation of motion is

$$\boldsymbol{M}.\ddot{\boldsymbol{q}} + \boldsymbol{K}.\boldsymbol{q} = \boldsymbol{0} \tag{20}$$

Finally, the approximation of the eigenfrequencies $f_{mod}^{(i)}$ and the mode shapes $\mathcal{F}_i(\boldsymbol{\phi}^{(i)}, x)$ are obtained by solving the generalized eigenvalues problem,

$$\left(\boldsymbol{K} - \left(2 \cdot \pi \cdot f_{mod}^{(i)}\right)^2 \boldsymbol{M}\right)\boldsymbol{\phi}^{(i)} = \boldsymbol{0} \tag{21}$$

3.5. Model Validation

3.5.1. Characteristics of the Reference Tower

To evaluate the Rayleigh–Ritz model's capacity to estimate the tower's dynamic properties, a referenced case computed with a 3D finite element model is considered. The finite element code Cast3M has been used for this study. The 3D FE model of the tower is composed of 104,400 elements and 122,500 nodes. A total of 700 nodes are involved in the SSI, and 2368 nodes in the interaction with an adjacent structure. Three degrees of freedom per node are used. Additional stiffness and displacement boundary conditions are managed by dual Lagrange multipliers. Figure 14a gives the mesh of the reference computation made with the finite element code Cast3M [196], (see: http://www-cast3m.cea.fr/ accessed on 1 October 2021).

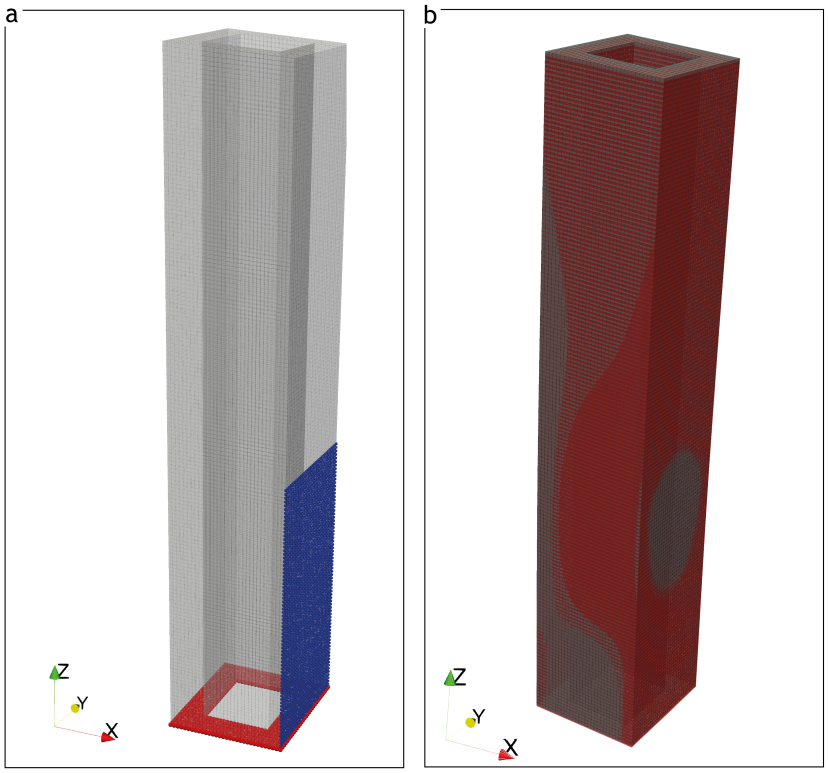

Figure 14. (**a**) 3D finite element model of the reference bell tower (red dots—SSI multiaxial springs, blue dots—TNI monoaxial springs along the direction *X*). (**b**) Comparison of the mode shape for the first bending mode between the reference 3D FE model (red) and the Rayleigh–Ritz model (gray).

The geometric and material characteristics considered for the tower are: H = 17.6 m (isolated tower), H = 35 m (bounded tower), l_s = 7.39 m (isolated tower), l_s = 6.17 m (bounded tower), $L_s = 1.01 \cdot \ell_s$, $t_w = 0.2 \cdot \ell_s$, E = 2.2 GPa, $\nu = 0.2$, $\rho = 1800$ kg/m^3, $k_s = 10^7$ N/m, $k_r = 10^8$ N·m, $k_n = 10^8$ N/m^2, $h_n = 0.42 \cdot H$, $M_b = 2600$ kg, and $h_b = H$. Except for the soil, these values correspond to the median values in the database.

3.5.2. Evaluation of the Error

The consistency can be evaluated by comparing the frequencies:

$$\Delta f\left(f_{mod}^{(i)}, f_{FE}^{(i)}\right) = \frac{f_{FE}^{(i)} - f_{mod}^{(i)}}{f_{FE}^{(i)}} \tag{22}$$

The degree of consistency between the mode shapes of the Rayleigh–Ritz model $f_{mod}^{(i)}$ and the ones of the finite element reference $f_{FE}^{(i)}$ can be measured with the Modal Assurance Criterion (MAC),

$$MAC\left(f_{mod}^{(i)}, f_{FE}^{(j)}\right) = \frac{\left[\boldsymbol{f}_{mod}^{(i)}(\boldsymbol{x}_p)\right]^T \boldsymbol{f}_{FE}^{(j)}(\boldsymbol{x}_p)}{\left(\left[\boldsymbol{f}_{mod}^{(i)}(\boldsymbol{x}_p)\right]^T \boldsymbol{f}_{mod}^{(i)}(\boldsymbol{x}_p)\right)\left(\left[\boldsymbol{f}_{FE}^{(j)}(\boldsymbol{x}_p)\right]^T \boldsymbol{f}_{FE}^{(j)}(\boldsymbol{x}_p)\right)} \tag{23}$$

where $\boldsymbol{x}_p$ is the set of points for which the mode shapes are computed. From the MAC, one can define an error Δ_{MAC} as

$$\Delta_{MAC} = \frac{1}{N_m} \sum_{i=1}^{N_m} \left[1 - MAC\left(f_{mod}^{(i)}, f_{FE}^{(i)}\right)\right] \tag{24}$$

where N_m is the number of modes considered.

3.5.3. Results

Three cases are considered to evaluate the capacity of the Rayleigh–Ritz model to describe the dynamic properties of slender structures: (1) a fixed base without interaction with the nave, (2) a fixed base with interaction with the nave, and (3) soil–structure interaction and nave interaction.

Table 8 gives the three first eigenfrequencies for global bending modes along the direction X in the three case studies.

Table 8. Evaluation of the eigenfrequencies using the Rayleigh–Ritz model. Case 1: fixed base without interaction with the nave. Case 2: fixed base with interaction with the nave. Case 3: soil–structure interaction and nave interaction.

	Case 1			**Case 2**			**Case 3**		
Mode	f_{FE} **[Hz]**	f_{mod} **[Hz]**	Δf **[%]**	f_{FE} **[Hz]**	f_{mod} **[Hz]**	Δf **[%]**	f_{FE} **[Hz]**	f_{mod} **[Hz]**	Δf **[%]**
1	2.40	2.39	0.42	4.88	4.87	0.2	4.49	4.40	2.00
2	12.26	12.27	0.08	15.83	16.00	1.07	11.77	11.74	0.25
3	28.27	28.34	0.02	29.76	29.92	0.54	16.80	16.31	2.92

An excellent estimation is obtained for the eigenfrequencies for the three case studies with relative errors lower than 3%.

To compute the MAC between the modal basis of the Rayleigh–Ritz model and the reference with volumic finite element, the mode shapes should be described on the same set

of point $\boldsymbol{x}_p$. The mode shapes obtained with the Rayleigh–Ritz model are thus considered to move the nodes of the 3D finite element mesh by using the beam kinematic,

$$u_X\left(x_p^i\right) = v\left(X\left(x_p^i\right)\right), \quad u_Y\left(x_p^i\right) = 0, \quad u_Z\left(x_p^i\right) = -Z(x_p^i) \cdot \theta\left(X\left(x_p^i\right)\right) \tag{25}$$

Figure 14b compares the mode shape of the first mode for the third case study between the finite Element reference and the Rayleigh–Ritz model. The two mode shapes appeared similar. The non-consideration of the Poisson effect with the beam model can explain the slight discrepancy.

Figure 15 gives the MAC matrix obtained for the three case studies regarding the three first bending modes in the X direction.

The MAC error Δ_{MAC} between the three first bending modes of the Rayleigh–Ritz model and the reference FE model in the X direction for the three case studies are $\Delta_{MAC}^{(1)} = 13.32\%$, $\Delta_{MAC}^{(2)} = 15.36\%$, $\Delta_{MAC}^{(3)} = 12.93\%$. The slight difference between the two models expressed in terms of eigenfrequency and MAC error highlights the Rayleigh–Ritz model's efficiency in describing the system's main dynamic properties, considering local features and interaction.

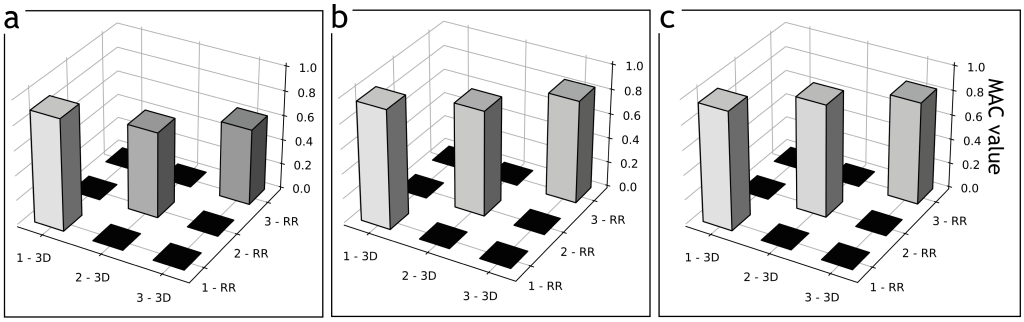

Figure 15. Modal Assurance Criterion matrix with the three first modes of the 3D finite element model (3D) and the Rayleigh–Ritz model (RR). (**a**) Case 1: fixed base without interaction with the nave. (**b**) Case 2: fixed base with interaction with the nave. (**c**) Case 3: soil–structure interaction and nave interaction.

3.6. Sensitivity Analysis

In this last part, sensitivity analyses are performed to quantify the contribution of each of the parameters on the dynamic properties of the Rayleigh–Ritz model. This analysis aims to identify the main parameters influencing the fundamental frequency estimation. It aims to help identify the main parameters to measure on an actual structure when characterizing the dynamic properties of the structure with the model.

3.6.1. The FAST Method

Global sensitivity analysis is a method used to decompose the uncertainty in the output of a computational model according to the input sources of uncertainty [197]. In this kind of sensitivity analysis, the space of the input factors is explored within an infinite region [198].

The Fourier amplitude sensitivity test (FAST), [198,199] and the Random balance designs Fourier amplitude sensitivity test (RBD-FAST) [200,201] are some of the most robust global sensitivity analysis techniques, e.g., [201–204]. This last technique sampled all input parameters from a periodic function with a different characteristic frequency. Thus, the output model becomes a periodic function. The Fourier spectrum is then calculated on the model output at specific frequencies to obtain the first-order Sobol sensitivity index (S_i) of each p_i parameter.

Let us consider a computer model $Y = \mathcal{M}(p_1, \ldots, p_n)$ treated as a black box, where n is the number of independent input parameters. The parametric curve assigned to each input parameter is defined as:

$$p_i(s) = \frac{1}{2} + \frac{1}{\pi} \arcsin(\sin(w_i \cdot s)) \tag{26}$$

where $p_i(s) \in [0,1]^n$ and $s = 2 \cdot \pi \frac{j-1}{N}; \forall j = 1, \ldots, N$. The Y model is then evaluated N times over the sample of size N. If the model output Y is expanded with a Fourier series, the marginal variance (V) can be obtained as:

$$\mathcal{M}_0 = E[Y] \tag{27}$$

$$\mathcal{M}_0 = \lim_{T \to \infty} \frac{1}{2\pi} \int_{-\pi}^{\pi} f(\mathrm{p(s)}) ds \tag{28}$$

$$V = \frac{1}{2\pi} \int_{-\pi}^{\pi} \mathcal{M}^2(\mathrm{p(s)}) ds - \mathcal{M}_0^2 \tag{29}$$

$$V \simeq 2 \sum_{j=1}^{\infty} (A_j^2 + B_j^2) \tag{30}$$

where A_j and B_j are the Fourier coefficients defined as:

$$A_j = \frac{1}{2\pi} \int_{-\pi}^{\pi} \mathcal{M}(\mathrm{p(s)}) \cos(js) ds \tag{31}$$

$$B_j = \frac{1}{2\pi} \int_{-\pi}^{\pi} \mathcal{M}(\mathrm{p(s)}) \sin(js) ds \tag{32}$$

The marginal partial variance of an individual input parameter (V_i) is obtained from the Fourier coefficients A_{kw_i} and B_{kw_i} at the harmonics of w_i as follows:

$$V_i = 2 \sum_{k=1}^{\infty} (A_{kw_i}^2 + B_{kw_i}^2) \tag{33}$$

Finally, the first-order Sobol index (S_i) of each p_i parameters is defined as:

$$S_i = \frac{V_i}{V} \tag{34}$$

The number of simulations N_s needed in FAST and the ω_i values for Equation (26) are provided in Table 9. It is noted that even for a problem with a few numbers of input variables, the minimum number of simulations required to obtain reliable data is high.

The advantage of RBD-FAST is that each random variable may be sampled from a periodic search function considering a single frequency w_i for all input variables, which will reduce the number of simulations N_s. However, only the first-order sensitivity index (S_i) could be calculated. This is possible thanks to a randomization procedure used in RBD-FAST [201]. The randomization procedure consists of the following:

- Randomly permutes the set of samples for each input variable;
- Run the model using those permuted sets of input variables;
- Reorder the model output according to the input permutation for each input variable.

Then, for each reordered output set, the single frequency w_i is restored, and the sensitivity indices may be evaluated using the same procedure as in FAST. The reader may refer to [198,201,204,205] or [206], among others, for further details about the FAST and RBD-FAST methods.

Table 9. Minimum number of model runs required by FAST [198].

Input Factors	N_s	ω_i
5	626	$\{11, 21, 27, 35, 39\}$
6	786	$\{1, 21, 31, 37, 45, 49\}$
7	1394	$\{17, 39, 59, 69, 75, 83, 87\}$
$N_s = (2 \cdot M \cdot \omega_{max} + 1) \cdot 2$		

3.6.2. Sensitivity Analysis of the Rayleigh–Ritz Model

The first-order Sobol indices [207] are computed for the case of bounded towers without soil–structure interaction and with a rectangular hollow section. For this computation, a combination of the Random Balance Design (RBD) and the Fourier Amplitude Sensitivity Analysis Test (FAST) [200] is used. The sampling is made by considering Latin Hypercube Sampling (LHS). These analyses have been made with the Python library SALib [208].

Table 10 lists the range of the values for the different parameters. The ranges have been constructed according to the descriptive statistics of the database in the first part of this work.

Table 10. Range of values for the parameters of the Rayleigh–Ritz approach for the sensitivity analysis.

Parameters [Unit]	Range
H [m]	13.1–56.8
ℓ_s [m]	3.2–10.2
$\frac{t_w}{\ell_s}$ [%]	100–130
$\frac{L_s}{\ell_s}$ [%]	25–36
E [GPa]	0.2–5.3
ν [-]	0.13–0.27
ρ [kg·m^{-3}]	1500–2100
$\frac{h_n}{H}$ [%]	25–59
k_n [N·m^2]	10^4–10^9
M_b [kg]	0–6500

The first-order Sobol indices are computed for the fundamental frequency associated with the first bending mode. Figure 16 gives these first-order Sobol indices with a confidence interval.

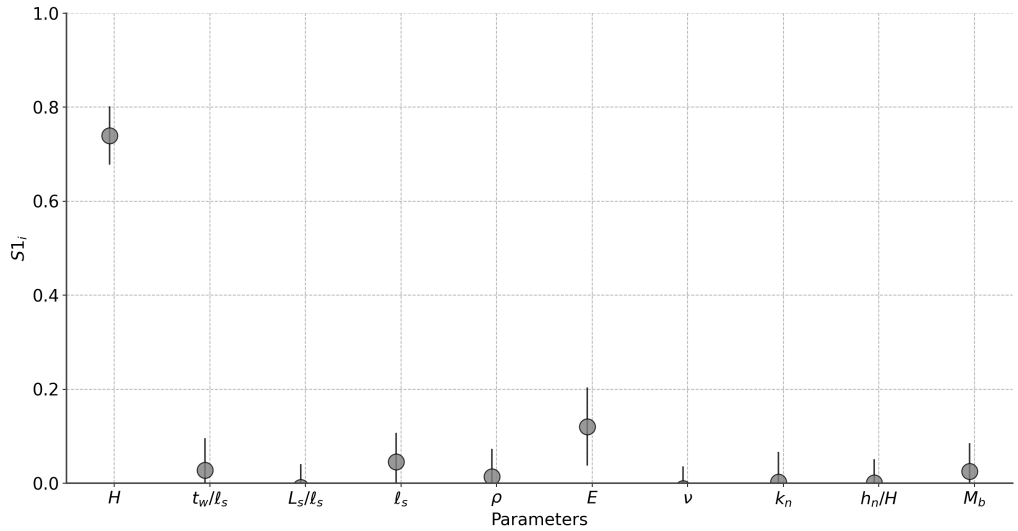

Figure 16. First-order Sobol indices for the fundamental frequency associated with bending mode regarding nine parameters for the Rayleigh–Ritz model.

Figure 16 shows that the fundamental frequency is mainly sensitive to the tower's height (S_1 = 0.74). This result justifies the choice of H as the single or as one of the parameters for the empirical models. This shows that particular care needs to be taken when evaluating this parameter to minimize the fundamental frequency evaluation error. The modulus of elasticity plays a second-order role (S_1 = 0.12). The width and height of the interaction between the bell tower and the nave have a lesser impact, but can be used to refine the evaluation of the fundamental frequency (to a hundredth of a Hz).

However, the impact of characteristics other than height on the fundamental frequency can vary according to the height range of the structure. To assess this, the Sobol index of each parameter is evaluated as a function of the tower's height. The sensitivity analysis was carried out using interval values for the nine parameters as shown in Table 10. Figure 17 (on the left) shows a decreasing contribution of Young's modulus with increasing height. On the contrary, the interaction height between the tower and adjacent buildings increases proportionally with the height. The other parameters have a more constant and minor role in the selected range of values (Figure 17, on the right).

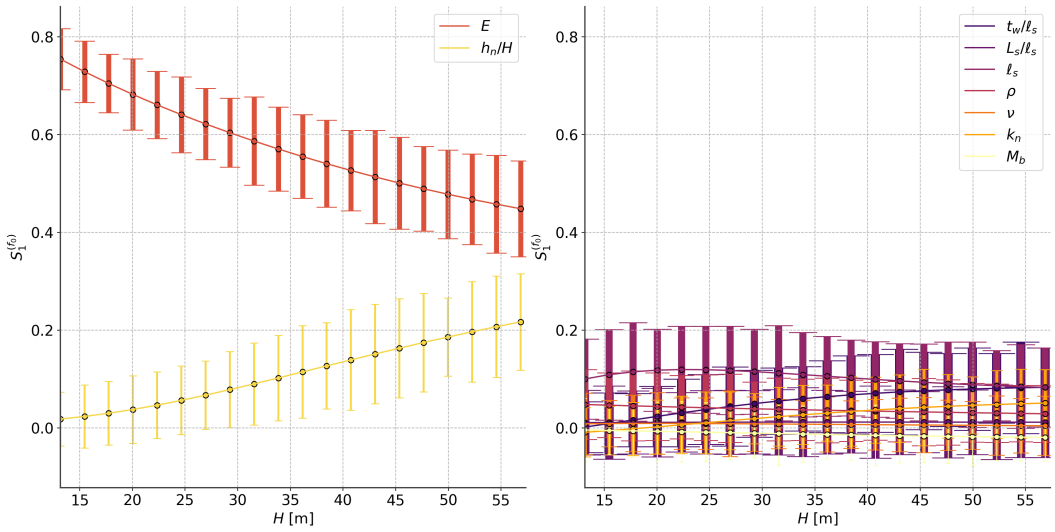

Figure 17. Evolution of the first-order Sobol indices of the towers features with respect to the height H of the tower.

3.6.3. Sensitivity Analysis for Key Parameter Identification

This section proposes to go a step further and quantify the impact of errors in field measurements of geometric characteristics and material properties on the modal frequencies and strains of the first three bending modes of the tower evaluated using the Rayleigh–Ritz approach. To do this, we use a numerical framework. A 3D Finite Element Model is used as a reference model (Figure 15, on the left). The value of geometric and material characteristics considered are the same as those of the bounded tower discussed in Section 3.5.1 (height, wall thickness, width, length, density, interface stiffness, and height). The Rayleigh–Ritz approach is used to propagate the errors of nine parameters: t_w, ℓ_s, L_s, ρ, E, ν, k_s, h_n, and M_b. The tower's height is kept fixed. To simulate the error, each parameter varies between plus and minus 10 % of the reference value. The consistency between the frequencies and the modes shapes identified with the Rayleigh–Ritz approach and the reference 3D Finite Element Model is evaluated through $\Delta_{f_i}(\boldsymbol{p})$ and $\Delta_{MAC_i}(\boldsymbol{p})$, as defined in Equation (22) and Equation (23), respectively. The first-order Sobol indices are computed, and results are shown in Figure 18. The breath measurement error contributes most to the mode shape error of the first three modes. The density and the Young modulus uncertainties impact higher frequencies (the second and third bending modes). The measurement error on the interaction height mainly affects the fundamental frequencies and their associated mode shape.

3.7. Comparing Empirical, Physics-Based, and Rayleigh–Ritz Approach for the Evaluation of the Fundamental Frequency

In this final section, we compare the performance of the empirical, physics-based, and Rayleigh–Ritz approaches for evaluating the fundamental frequency of slender historical structures. The analysis is carried out on a set of towers for which the geometric characteristics, the mass of the bell system, and the material properties are available (31 towers). Figure 19 shows the results expressed in terms of residuals computed as follows: $\frac{f_0^{exp} - f_0^{model}}{f_0^{exp}}$. The physics-based formulations constantly underestimate the experimental frequency. This discrepancy could be related to the value of the selected material parameters found in the literature, primarily identified through the FE model updating processes. The results of the empirical formulation are spread out, and failed to minimize the discrepancy between the estimated and the experimental frequencies. This result is consistent with those shown in Figures 10 and 12. On the contrary, the figure clearly shows that the Rayleigh–Ritz model minimizes the best deviation from the measured frequency. However, this difference does not converge to zero, and this can be explained by several factors. Sensitivity analyses show that the tower's height impacts the fundamental frequency most. This height is often defined with precision about decimeters, or even meters in some cases, and could explain these discrepancies. In addition, the presence of complex and imposing roofs (sometimes made of wood, sometimes of masonry) complicates the definition of the height to be retained. It has been observed that a low value (height at the base of the roof) and a high value (height at the top of the roof) systematically frame the value of the experimental frequency. The presence of an opening in the roof can also have a significant impact by significantly reducing the mass. The material parameters also need to be better known. These are often the result of updating the process with a finite element model that is more complex than the model considered in this study. However, the model proposed here remains a reasonable compromise, given the uncertainties in masonry towers' physical and geometric parameters.

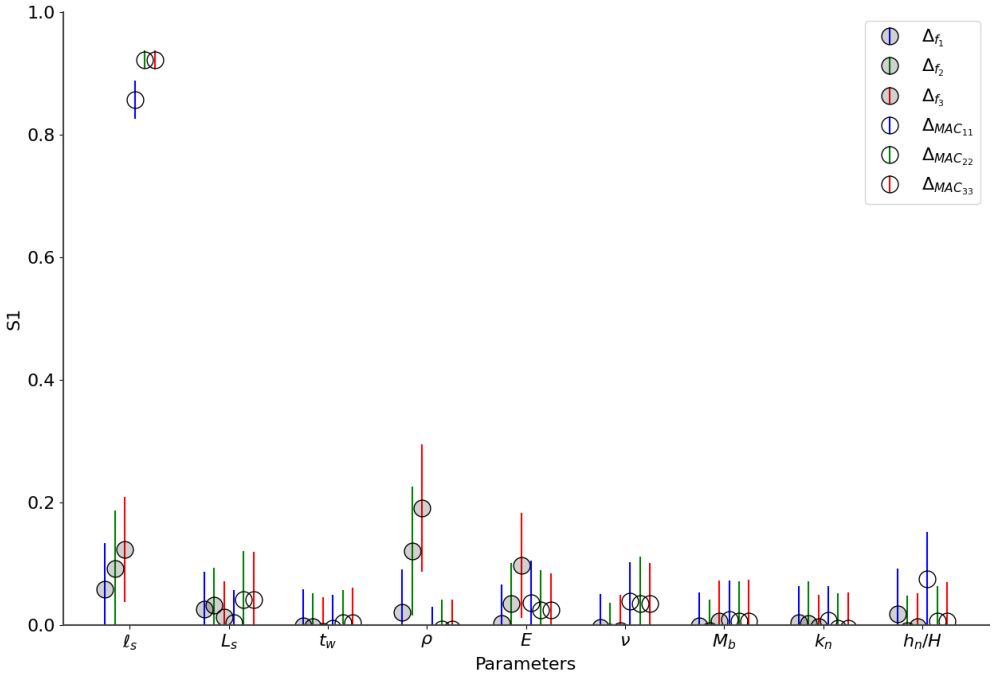

Figure 18. Evaluation of the first-order Sobol indices for the errors regarding the dynamic properties.

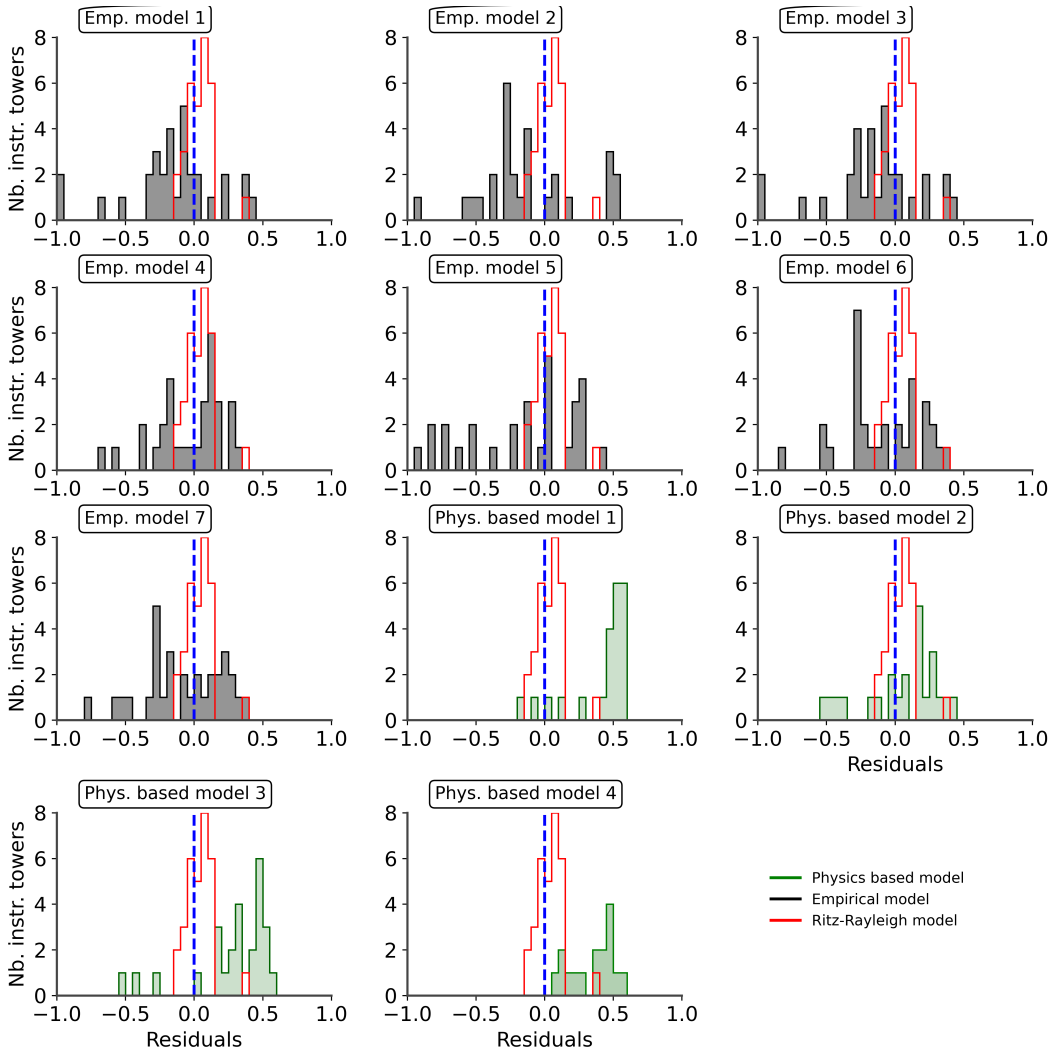

Figure 19. Comparison of the fundamental frequency residuals using empirical formulation (gray), physics-based formulation (green), and the Rayleigh–Ritz approach (red).

4. Conclusions

The fundamental frequency is crucial in assessing slender masonry structures' dynamic properties. In recent decades, simple formulations have been proposed based on global features avoiding difficult and time-consuming modeling. At the same time, the growing number of OMA campaigns provides information on actual modal characteristics, and this is an opportunity to revisit and investigate the behavior of old masonry structures. This work's contributions are:

- Compiling 244 instrumented masonry towers assembled from an extensive literature review. Worldwide masonry towers are described in terms of geometric, material features, interaction with adjacent buildings, aging, construction phase, repairs, and instrumentation condition;
- Describing the range of each parameter essential for the sensitivity analysis;
- Proposing a generic formulation for empirical and physical models summarizing the ones from the literature (available in the Python script);
- Expressing each feature contribution through a Rayleigh–Ritz formulation (available in the Python script);
- Conducting a sensitivity analysis to quantify how much each feature's tower impacts the fundamental frequency.

The main results of this work show that:

- The variability of the identified experimentally for the same historic tower. When available, most of the repeated OMA surveys highlight a discrepancy of up to 0.05 Hz. This difference is in the range of the contribution of tower features, inviting us to reduce in the uncertainties when evaluating both the fundamental frequency and the tower's features;
- Empirical relations provide a suitable evaluation of the fundamental frequency compared to physics-based formulations regarding a small number of parameters;
- The Rayleigh–Ritz formulation allows the best fit between experimental and computed fundamental frequency when all information about the towers' features are available;
- The height of the tower is the critical parameter to evaluate the fundamental frequency. It invites us to take some precautions when evaluating the height of the building. Moreover, the impact of the interaction between the slender structure and the adjacent structure on the fundamental frequency increase with the tower's height, although as a second-order parameter;
- The width significantly impacts the mode shapes of the three first bending modes. The density and Young modulus impact the frequencies of the second and higher modes. The impact of the height interaction is limited to the first bending modes. The tower's other features play a second-order role. These values are generally taken as known in model updating processes, which prefer to focus on calibrating unknown material properties. They are measured by visual inspection or more advanced techniques (laser measurements, etc.). We recommend particular attention to minimizing the uncertainty associated with measuring these two parameters.

Cultural Heritage buildings are complex, but of inestimable value, which requires our synergy. We believe this work is an initial contribution that invites sharing data relating to OMA (the fundamental frequency in the first instance). The database and the script of this work are available to the community. We encourage the community to send us the characteristics of new instrumented masonry towers so that we can increase our understanding of their behavior and work towards their preservation.

Author Contributions: Conceptualization, A.M. and C.G.; Methodology, A.M., C.G., E.D.M. and P.G.; Software, A.M. and C.G.; Validation, A.M. and C.G.; Formal analysis, A.M., C.G., J.L. and C.C.; Investigation, A.M., C.G. and C.L.S.; Resources, C.G.; Data curation, A.M., C.G., C.L.S., J.L. and C.C.; Writing—original draft, A.M. and C.G.; Writing—review & editing, A.M., C.G., C.L.S., E.D.M. and P.G.; Visualization, A.M. and C.G.; Supervision, A.M. and C.G.; Project administration, C.G.; Funding acquisition, C.G. All authors have read and agreed to the published version of the manuscript.

Funding: The first, the second, and the sixth author wish to express their most grateful thanks to the French National Research Agency (ANR) for the funding of the ACROSS project (ANR-20-CE03–0003), through which a part of this study has been carried out.

Data Availability Statement: The code sources and the TURRIS are provided at the following link: https://github.com/MArnaud/TURRIS [16].

Acknowledgments: The authors kindly acknowledge the institutions and researchers who provided additional and helpful information of masonry towers features: the municipality of Montboucher-sur-Jabron. The authors thanks Fernando Lopez-Caballero for the fruitful discussion and the advice regarding the sensitivity analysis, Clotilde Chambreuil and Héloïse Rostagni for their help in completing the database. The authors wish to express their most grateful thanks to the French National Research Agency (ANR) for the funding of the ACROSS project (ANR-20-CE03–0003), through which a part of this study has been carried out.

Conflicts of Interest: The authors declare no conflict of interest.

References

1. Shakya, M.; Varum, H.; Vicente, R.; Costa, A. Empirical formulation for estimating the fundamental frequency of slender masonry structures. *Int. J. Archit. Herit.* **2016**, *10*, 55–66. [CrossRef]
2. Bartoli, G.; Betti, M.; Marra, A.M.; Monchetti, S. On the role played by the openings on the first frequency of historic masonry towers. *Bull. Earthq. Eng.* **2020**, *18*, 427–451. [CrossRef]
3. Pallarés, F.J.; Betti, M.; Bartoli, G.; Pallarés, L. Structural health monitoring (SHM) and Nondestructive testing (NDT) of slender masonry structures: A practical review. *Constr. Build. Mater.* **2021**, *297*, 123768. [CrossRef]
4. Milani, G.; Casolo, S.; Naliato, A.; Tralli, A. Seismic Assessment of a Medieval Masonry Tower in Northern Italy by Limit, Nonlinear Static, and Full Dynamic Analyses. *Int. J. Archit. Herit.* **2012**, *6*, 489–524. [CrossRef]
5. DPCM. *Direttiva del Presidente del Consiglio dei Ministri per Valutazione e Riduzione del Rischio Sismico del Patrimonio Culturale con Riferimento alle Norme Tecniche per le Costruzioni, G.U. n. 47*; DPCM: Roma, Italy, 2011.
6. Brincker, R.; Ventura, C. *Introduction to Operational Modal Analysis*; John Wiley & Sons: Hoboken, NJ, USA, 2015.
7. Lund, J.; Selby, A.; Wilson, J. The dynamics of bell towers—A survey in northeast England. *WIT Trans. Built Environ.* **1995**, *17*, 8.
8. Bartoli, G.; Betti, M.; Marra, A.M.; Monchetti, S. Semiempirical Formulations for Estimating the Main Frequency of Slender Masonry Towers. *J. Perform. Constr. Facil.* **2017**, *31*. [CrossRef]
9. Sanchez-Silva, M.; Klutke, G.A.; Rosowsky, D.V. Life-cycle performance of structures subject to multiple deterioration mechanisms. *Struct. Saf.* **2011**, *33*, 206–217. [CrossRef]
10. Price Code. *Eurocode 8: Design of Structures for Earthquake Resistance—Part 1: General Rules, Seismic Actions and Rules for Buildings*; European Committee for Standardization: Brussels, Belgium, 2005.
11. Faccio, P.; Podestà, S.; Saetta, A. Venezia, Campanile della Chiesa di Sant'Antonin, Esempio 5. In *Linee Guida per la Valutazione e Riduzione del Rischio Sismico del Patrimonio Culturale Allineate alle Nuove Norme Tecniche per le Costruzioni (DM 14/01/2008), Circolare*; Ministero della Cultura: Rome, Italy, 2011; Volume 26.
12. Rainieri, C.; Fabbrocino, G. Estimating the Elastic Period of Masonry Towers. In *Topics in Modal Analysis I*; Springer: New York, NY, USA, 2012; Volume 5, pp. 243–248. [CrossRef]
13. Diaferio, M.; Foti, D.; Potenza, F. Prediction of the fundamental frequencies and modal shapes of historic masonry towers by empirical equations based on experimental data. *Eng. Struct.* **2018**, *156*, 433–442. [CrossRef]
14. Ministerio de Fomento. Real Decreto 997/2002, de 27 de septiembre, por el que se aprueba la norma de construcción sismorresistente: Parte general y edificación (NCSR-02). Boletín Oficial del Estado , 11 October 2002.
15. Formisano, A.; Vituat, R.; Milani, G.; Sarhosis, V. *Parametric Seismic Analysis on Masonry Bell Towers*; Pisa University Press: Pisa, Italy, 2017; pp. 108–116.
16. Montabert, A.; Giry, C.; Limoge Schraen, C.; Lépine, J.; Choueiri, C.; Mercerat, E.D.; Guéguen, P. TURRIS: An open source database and Python tools to compute the fundamental frequency of historic masonry towers. *Zenodo* **2023**. Available online: https://zenodo.org/record/8283641 (accessed on 18 August 2023).
17. Schmidt, T. Dynamic behaviour of twin bell towers. In Proceedings of the 2nd International Operational Modal Analysis Conference, Copenhagen, Denmark, 30 April–2 May 2007.
18. Schmidt, T. FE Comparison of the dynamic behavior of 16 historical twin bell towers. In Proceedings of the 3th International Operational Modal Analysis Conference, Portonovo, Italy, 4–6 May 2009; pp. 483–490.
19. Rainieri, C.; Fabbrocino, G. Output-only modal identification for prediction of the elastic period of masonry towers. In Proceedings of the 4th International Operational Modal Analysis Conference, Istanbul, Turkey, 9–11 May 2011.
20. Limoge, C. Méthode de Diagnostic à Grande Échelle de la Vulnérabilité Sismique des Monuments Historiques: Chapelles et Églises Baroques des Hautes Vallées de Savoie: Large-Scale Seismic Vulnerability Assesment Method for the Masonry Architectural Heritage: Baroque Chapels and Churches of the French Savoye. Ph.D. Thesis, Université Paris-Saclay (ComUE), Paris, France, 2016.
21. Ziegler, A. Dynamik der Glockentürme. In *Bauwerksdynamik und Erschütterungsmessungen*; Springer Fachmedien: Wiesbaden, Germany, 2017; pp. 153–165. [CrossRef]
22. Ruiz-Jaramillo, J.; Montiel-Vega, L.; García-Pulido, L.J.; Muñoz-González, C.; Blanca-Hoyos, Á. Ambient Vibration as a Basis for Determining the Structural Behaviour of Watchtowers against Horizontal Loads in Southeast Spain. *Appl. Sci.* **2020**, *10*, 6114. [CrossRef]
23. Mercerat, D.; Montabert, A.; Giry, C.; Lancieri, M.; Arrighetti, A. Operational Modal Analysis of five historical bell towers in the Mugello basin (Tuscany, Italy). In Proceedings of the 3rd European Conference on Earthquake Engineering & Seismology (3ECEES), Bucharest, Romania, 4–9 September, 2022; pp. 4106–4111.
24. Wimmer, H.; Majer, J. Dynamic behaviour and numerical simulation of old bell towers. In *Structural Repair and Maintenance of Historical Buildings*; Computational Mechanics Publications: Berlin, Germany, 1989; pp. 349–358.
25. Modena, C.; Valluzzi, M.; Folli, R.T.; Binda, L. Design choices and intervention techniques for repairing and strengthening of the Monza cathedral bell-tower. *Constr. Build. Mater.* **2002**, *16*, 385–395. [CrossRef]
26. Ivorra, S.; Foti, D.; Diaferio, M.; Carabellese, I. Preliminary OMA results on a soft calcarenite stone bell-tower in Mola di Bari (Italy). In Proceedings of the 7th International Operational Modal Analysis Conference, IOMAC, Ingolstadt, Germany, 10–12 May 2017.

27. Combey, A.; Mercerat, D.E.; Gueguen, P.; Langlais, M.; Audin, L. Postseismic Survey of a Historic Masonry Tower and Monitoring of Its Dynamic Behavior in the Aftermath of Le Teil Earthquake (Ardèche, France). *Bull. Seismol. Soc. Am.* **2022**, *112*, 1101–1119. [CrossRef]
28. Kohan, P.H.; Nallim, L.G.; Gea, S.B. Dynamic characterization of beam type structures: Analytical, numerical and experimental applications. *Appl. Acoust.* **2011**, *72*, 975–981. [CrossRef]
29. Carone, A.S.; Foti, D.; Giannoccaro, N.I.; Nobile, R. Non-destructive characterization and dynamic identification of an historical bell tower. In Proceedings of the 4th International Conference on Integrity, Reliability and Failure, Funchal, Portugal, 23–27 June 2013; pp. 1–16.
30. Diaferio, M.; Foti, D.; Giannoccaro, N. Modal parameters identification on environmental tests of an ancient tower and validation of its FE model. *Int. J. Mech* **2016**, *10*, 80–89.
31. Mariella, D.; Dora, F.; Gentile, C.; Ivan Giannoccaro, N.; Saisi, A.E. Dynamic testing of a historical slender building using accelerometers and radar. In Proceedings of the 6th International Operational Modal Analysis Conference, Gijón, Spain, 12–14 May 2015; pp. 1–10.
32. Stefano, A.D.; Ceravolo, R. Assessing the Health State of Ancient Structures: The Role of Vibrational Tests. *J. Intell. Mater. Syst. Struct.* **2007**, *18*, 793–807. [CrossRef]
33. Lucidi, A.; Giordano, E.; Clementi, F.; Quattrini, R. Point cloud exploitation for structural modeling and analysis: A reliable workflow. *Int. Arch. Photogramm. Remote Sens. Spat. Inf. Sci.* **2021**, *XLIII-B2-2021*, 891–898. [CrossRef]
34. Gentile, C.; Saisi, A. Operational modal testing of historic structures at different levels of excitation. *Constr. Build. Mater.* **2013**, *48*, 1273–1285. [CrossRef]
35. Gentile, C.; Saisi, A.; Cabboi, A. Structural Identification of a Masonry Tower Based on Operational Modal Analysis. *Int. J. Archit. Herit.* **2014**, *9*, 98–110. [CrossRef]
36. Cabboi, A.; Gentile, C.; Saisi, A. From continuous vibration monitoring to FEM-based damage assessment: Application on a stone-masonry tower. *Constr. Build. Mater.* **2017**, *156*, 252–265. [CrossRef]
37. Ferraioli, M.; Mandara, A.; Abruzzese, D.; Miccoli, L. Dynamic identification and seismic safety of masonry bell towers. In Proceedings of the 14th Conference of Associazione Nazionale Italiana di Ingegneria Sismica (ANIDIS), Bari, Italy, 18–22 September 2011; pp. 18–22.
38. Angelis, A.D.; Lourenço, P.B.; Sica, S.; Pecce, M.R. Influence of the ground on the structural identification of a bell-tower by ambient vibration testing. *Soil Dyn. Earthq. Eng.* **2022**, *155*, 107102. [CrossRef]
39. Pesci, A.; Teza, G.; Bonali, E.; Casula, G.; Boschi, E. A laser scanning-based method for fast estimation of seismic-induced building deformations. *ISPRS J. Photogramm. Remote Sens.* **2013**, *79*, 185–198. [CrossRef]
40. Palermo, M.; Silvestri, S.; Gasparini, G.; Baraccani, S.; Trombetti, T. An approach for the mechanical characterisation of the Asinelli Tower (Bologna) in presence of insufficient experimental data. *J. Cult. Herit.* **2015**, *16*, 536–543. [CrossRef]
41. Carpinteri, A.; Lacidogna, G.; Manuello, A.; Niccolini, G. A study on the structural stability of the Asinelli Tower in Bologna. *Struct. Control. Health Monit.* **2015**, *23*, 659–667. [CrossRef]
42. Invernizzi, S.; Lacidogna, G.; Lozano-Ramírez, N.E.; Carpinteri, A. Structural monitoring and assessment of an ancient masonry tower. *Eng. Fract. Mech.* **2019**, *210*, 429–443. [CrossRef]
43. Milani, G.; Clementi, F. Advanced Seismic Assessment of Four Masonry Bell Towers in Italy after Operational Modal Analysis (OMA) Identification. *Int. J. Archit. Herit.* **2019**, *15*, 157–186. [CrossRef]
44. Standoli, G.; Giordano, E.; Milani, G.; Clementi, F. Model Updating of Historical Belfries Based on Oma Identification Techniques. *Int. J. Archit. Herit.* **2020**, *15*, 132–156. [CrossRef]
45. Colapietro, D.; Fatiguso, F.; Pinto, M.; Bianco, F. Techniques for improving assessment of the seismic vulnerability of a masonry bell tower. *Am. J. Eng. Res. (AJER)* **2017**, *6*, 147–155.
46. Azzara, R.M.; Girardi, M.; Padovani, C.; Pellegrini, D. *Dynamic Behaviour of the Carillon Tower in Castel San Pietro, Italy*; Technical Report; ISTI: Rome, Italy, 2022.
47. Gazzani, V.; Poiani, M.; Clementi, F.; Milani, G.; Lenci, S. Modal parameters identification with environmental tests and advanced numerical analyses for masonry bell towers: A meaningful case study. *Procedia Struct. Integr.* **2018**, *11*, 306–313. [CrossRef]
48. Balduzzi, B.; Mazza, D.; Papis, D.; Rossi, C.; Rossi, P.P. Experimental and numerical analysis for the strengthening intervention of the bell tower of St. Sistós Church in Bergamo. In Proceedings of the 5th International Conference on Structural Analysis of Historical Constructions (SAHC), Delhi, India, 6–8 November 2006; pp. 6–8.
49. Girardi, M.; Padovani, C.; Pellegrini, D.; Robol, L. Model updating procedure to enhance structural analysis in FE code NOSA-ITACA. *J. Perform. Constr. Facil.* **2019**, *33*, 04019041. [CrossRef]
50. Casciati, S.; Al-Saleh, R. Dynamic behavior of a masonry civic belfry under operational conditions. *Acta Mech.* **2010**, *215*, 211–224. [CrossRef]
51. Casciati, S.; Faravelli, L. Vulnerability assessment for medieval civic towers. *Struct. Infrastruct. Eng.* **2010**, *6*, 193–203. [CrossRef]
52. D'Ambrisi, A.; Mariani, V.; Mezzi, M. Seismic assessment of a historical masonry tower with nonlinear static and dynamic analyses tuned on ambient vibration tests. *Eng. Struct.* **2012**, *36*, 210–219. [CrossRef]
53. Casciati, S.; Tento, A.; Marcellini, A.; Daminelli, R. Long run ambient noise recording for a masonry medieval tower. *Smart Struct. Syst.* **2014**, *14*, 367–376. [CrossRef]

54. Bianconi, F.; Salachoris, G.P.; Clementi, F.; Lenci, S. A Genetic Algorithm Procedure for the Automatic Updating of FEM Based on Ambient Vibration Tests. *Sensors* **2020**, *20*, 3315. [CrossRef] [PubMed]
55. Bassoli, E.; Vincenzi, L.; Bovo, M.; Mazzotti, C. Dynamic identification of an ancient masonry bell tower using a MEMS-based acquisition system. In Proceedings of the 2015 IEEE Workshop on Environmental, Energy, and Structural Monitoring Systems (EESMS), Trento, Italy, 9–10 July 2015. [CrossRef]
56. Bru, D.; Ivorra, S.; Betti, M.; Adam, J.M.; Bartoli, G. Parametric dynamic interaction assessment between bells and supporting slender masonry tower. *Mech. Syst. Signal Process.* **2019**, *129*, 235–249. [CrossRef]
57. Pieraccini, M.; Fratini, M.; Dei, D.; Atzeni, C. Structural testing of Historical Heritage Site Towers by microwave remote sensing. *J. Cult. Herit.* **2009**, *10*, 174–182. [CrossRef]
58. Pieraccini, M.; Dei, D.; Mecatti, D.; Parrini, F. Dynamic Testing of Historic Towers Using an Interferometric Radar from an Unstable Measurement Position. *J. Nondestruct. Eval.* **2013**, *32*, 398–404. [CrossRef]
59. Lacanna, G.; Ripepe, M.; Coli, M.; Genco, R.; Marchetti, E. Full structural dynamic response from ambient vibration of Giotto's bell tower in Firenze (Italy), using modal analysis and seismic interferometry. *NDT&E Int.* **2019**, *102*, 9–15. [CrossRef]
60. Ceravolo, R.; Pistone, G.; Fragonara, L.Z.; Massetto, S.; Abbiati, G. Vibration-Based Monitoring and Diagnosis of Cultural Heritage: A Methodological Discussion in Three Examples. *Int. J. Archit. Herit.* **2014**, *10*, 375–395. [CrossRef]
61. Camata, G.; Cifelli, L.; Spacone, E.; Conte, J.; Loi, M.; Torrese, P. Seismic Safety Assessment of the Tower of the S. Maria Maggiore Cathedral in Guardiagrele, Italy. In Proceedings of the Ninth International Conference on Computational Structures Technology, Athens, Greece, 2–5 September 2008. [CrossRef]
62. Capanna, I.; Cirella, R.; Aloisio, A.; Alaggio, R.; Fabio, F.D.; Fragiacomo, M. Operational Modal Analysis, Model Update and Fragility Curves Estimation, through Truncated Incremental Dynamic Analysis, of a Masonry Belfry. *Buildings* **2021**, *11*, 120. [CrossRef]
63. Buffarini, G.P.; Cimellaro, C.G.P.; Stefano, A.D. Experimental dynamic analysis of Palazzo Margherita in L'Aquila after the April 6th, 2009, Earthquake. In Proceedings of the Experimental Vibration Analysis for Civil Engineering Structures (EVACES), Varenna, Italy, 3–5 October 2011; pp. 247–254.
64. Peeters, B.; Sforza, G.; Sbaraglia, L.; Germano, F. Efficient operational modal testing and analysis for design verification and restoration baseline assessment: Italian case studies. In Proceedings of the Experimental Vibration Analysis for Civil Engineering Structures (EVACES), Varenna, Italy, 3–5 October 2011; pp. 3–5.
65. Barsocchi, P.; Bartoli, G.; Betti, M.; Girardi, M.; Mammolito, S.; Pellegrini, D.; Zini, G. Wireless Sensor Networks for Continuous Structural Health Monitoring of Historic Masonry Towers. *Int. J. Archit. Herit.* **2020**, *15*, 22–44. [CrossRef]
66. Zonta, D.; Pozzi, M.; Zanon, P.; Anese, G.; Busetto, A. Real-time probabilistic health monitoring of the Portogruaro Civic Tower. In *Structural Analysis of Historic Construction: Preserving Safety and Significance, Two Volume Set*; CRC Press: Boca Raton, FL, USA, 2008; pp. 743–752.
67. Azzara, R.M.; Roeck, G.D.; Girardi, M.; Padovani, C.; Pellegrini, D.; Reynders, E. The influence of environmental parameters on the dynamic behaviour of the San Frediano bell tower in Lucca. *Eng. Struct.* **2018**, *156*, 175–187. [CrossRef]
68. Barsocchi, P.; Cassara, P.; Mavilia, F.; Pellegrini, D. Sensing a city's state of health: Structural monitoring system by internet-of-things wireless sensing devices. *IEEE Consum. Electron. Mag.* **2018**, *7*, 22–31. [CrossRef]
69. Azzara, R.M.; Girardi, M.; Iafolla, V.; Padovani, C.; Pellegrini, D. Long-Term Dynamic Monitoring of Medieval Masonry Towers. *Front. Built Environ.* **2020**, *6*, 9. [CrossRef]
70. Saisi, A.; Gentile, C.; Guidobaldi, M. Post-earthquake continuous dynamic monitoring of the Gabbia Tower in Mantua, Italy. *Constr. Build. Mater.* **2015**, *81*, 101–112. [CrossRef]
71. Saisi, A.; Gentile, C. Post-earthquake diagnostic investigation of a historic masonry tower. *J. Cult. Herit.* **2015**, *16*, 602–609. [CrossRef]
72. Saisi, A.; Gentile, C.; Ruccolo, A. Pre-diagnostic prompt investigation and static monitoring of a historic bell-tower. *Constr. Build. Mater.* **2016**, *122*, 833–844. [CrossRef]
73. Gentile, C.; Guidobaldi, M.; Saisi, A. One-year dynamic monitoring of a historic tower: Damage detection under changing environment. *Meccanica* **2016**, *51*, 2873–2889. [CrossRef]
74. Cavalagli, N.; Comanducci, G.; Gentile, C.; Guidobaldi, M.; Saisi, A.; Ubertini, F. Detecting earthquake-induced damage in historic masonry towers using continuously monitored dynamic response-only data. *Procedia Eng.* **2017**, *199*, 3416–3421. [CrossRef]
75. Magrinelli, E.; Acito, M.; Bocciarelli, M. Numerical insight on the interaction effects of a confined masonry tower. *Eng. Struct.* **2021**, *237*, 112195. [CrossRef]
76. Gentile, C.; Saisi, A. Dynamic Testing of Masonry Towers Using the Microwave Interferometry. *Key Eng. Mater.* **2014**, *628*, 198–203. [CrossRef]
77. Saisi, A.; Terenzoni, S.; Ruccolo, A.; Gentile, C. Safety of the Architectural Heritage: Structural Assessment of the Zuccaro's Tower in Mantua. In *RILEM Bookseries*; Springer International Publishing: Berlin/Heidelberg, Germany, 2019; pp. 2422–2430. [CrossRef]
78. Fragonara, L.Z.; Boscato, G.; Ceravolo, R.; Russo, S.; Ientile, S.; Pecorelli, M.L.; Quattrone, A. Dynamic investigation on the Mirandola bell tower in post-earthquake scenarios. *Bull. Earthq. Eng.* **2016**, *15*, 313–337. [CrossRef]
79. Lancellotta, R.; Sabia, D. Identification Technique for Soil-Structure Analysis of the Ghirlandina Tower. *Int. J. Archit. Herit.* **2014**, *9*, 391–407. [CrossRef]

80. Foti, D.; Ivorra, S.; Sabbà, M.F. Dynamic Investigation of an Ancient Masonry Bell Tower with Operational Modal Analysis—Non-Destructive Experimental Technique to Obtain the Dynamic Characteristics of a Structure. *Open Constr. Build. Technol. J.* **2012**, *6*, 384–391. [CrossRef]
81. Clementi, F.; Pierdicca, A.; Formisano, A.; Catinari, F.; Lenci, S. Numerical model upgrading of a historical masonry building damaged during the 2016 Italian earthquakes: The case study of the Podestà palace in Montelupone (Italy). *J. Civ. Struct. Health Monit.* **2017**, *7*, 703–717. [CrossRef]
82. Saisi, A.; Gentile, C.; Ruccolo, A. Continuous monitoring of a challenging heritage tower in Monza, Italy. *J. Civ. Struct. Health Monit.* **2017**, *8*, 77–90. [CrossRef]
83. Lorenzoni, F.; Modena, C.; Caldon, M.; Cohen, M.; Kislev, R.; Schaffer, Y. Structural health monitoring of heritage sites: The tower of David in Jerusalem. In *Structural Analysis of Historical Constructions: Anamnesis, Diagnosis, Therapy, Controls*; CRC Press: Boca Raton, FL, USA, 2016; pp. 745–751. [CrossRef]
84. Montabert, A.; Mercerat, E.D.; Clément, J.; Langlaude, P.; Lyon-Caen, H.; Lancieri, M. High resolution operational modal analysis of Sant'Agata del Mugello in light of its building history. *Eng. Struct.* **2022**, *254*, 113767. [CrossRef]
85. Osmancikli, G.; Uçak, Ş.; Turan, F.N.; Türker, T.; Bayraktar, A. Investigation of restoration effects on the dynamic characteristics of the Hagia Sophia bell-tower by ambient vibration test. *Constr. Build. Mater.* **2012**, *29*, 564–572. [CrossRef]
86. Bayraktar, A.; Türker, T.; Sevım, B.; Altunişik, A.C.; Yildirim, F. Modal Parameter Identification of Hagia Sophia Bell-Tower via Ambient Vibration Test. *J. Nondestruct. Eval.* **2009**, *28*, 37–47. [CrossRef]
87. Cantieni, R. One-Year Monitoring of a Historic Bell Tower. *Key Eng. Mater.* **2014**, *628*, 73–78. [CrossRef]
88. Ivorra, S.; Pallarés, F.J.; Adam, J.M. Experimental and Numerical Results from the Seismic Study of a Masonry Bell Tower. *Adv. Struct. Eng.* **2009**, *12*, 287–293. [CrossRef]
89. Ivorra, S.; Pallarés, F.J. Dynamic investigations on a masonry bell tower. *Eng. Struct.* **2006**, *28*, 660–667. [CrossRef]
90. Ivorra, S.; Pallarés, F.J.; Adam, J.M.; Tomás, R. An evaluation of the incidence of soil subsidence on the dynamic behaviour of a Gothic bell tower. *Eng. Struct.* **2010**, *32*, 2318–2325. [CrossRef]
91. Ivorra, S.; Cervera, J.R. Analysis of the dynamic actions when bells are swinging on the bell tower of Bonreposi Mirambell Church (Valencia, Spain). In Proceedings of the 3rd international Seminar of Historical Constructions, Guimarães, Portugal, 7–9 November 2001; Volume 413, p. 19.
92. Cunha, Á.; Ramos, L.F.; Magalhães, F.; Lourenço, P.B. Dynamic identification and modelling of Clérigos Tower: Initial studies. In Proceedings of the EURODYN 2014—9th International Conference on Structural Dynamics, Porto, Portugal, 30 June–2 July 2014.
93. Ramos, L.; Marques, L.; Lourenço, P.; Roeck, G.D.; Campos-Costa, A.; Roque, J. Monitoring historical masonry structures with operational modal analysis: Two case studies. *Mech. Syst. Signal Process.* **2010**, *24*, 1291–1305. [CrossRef]
94. Guerreiro, L.; Azevedo, J. Análise e reforço da torres do relógio da Horta, Faial. In Proceedings of the 5th Encontro National de Sismologia e Engenharia Sismica. In Proceedings of the Encontro National de Sismologia e Engenharia Sismica, Azores, Portugal, 24–27 October 2001; pp. 639–650.
95. Júlio, E.N.B.S.; da Silva Rebelo, C.A.; da Costa, D.A.S.G.D. Structural assessment of the tower of the University of Coimbra by modal identification. *Eng. Struct.* **2008**, *30*, 3468–3477. [CrossRef]
96. Tomaszewska, A. Influence of statistical errors on damage detection based on structural flexibility and mode shape curvature. *Comput. Struct.* **2010**, *88*, 154–164. [CrossRef]
97. Tomaszewska, A.; Szymczak, C. Identification of the Vistula Mounting tower model using measured modal data. *Eng. Struct.* **2012**, *42*, 342–348. [CrossRef]
98. Shabani, A.; Ademi, A.; Kioumarsi, M. Structural Model Updating of a Historical Stone Masonry Tower in Tønsberg, Norway. In *Lecture Notes in Civil Engineering*; Springer International Publishing: Berlin/Heidelberg, Germany, 2021; pp. 576–585. [CrossRef]
99. Jaras, A.; Kliukas, R.; Kačianauskas, R. The dynamic loading of Vilnius archcathedral belfry–Investigation and analysis. In Proceedings of the 10th International Conference Modern Building Materials, Structures and Techniques, Vilnius, Lithuania, 19–21 May 2010.
100. Ribilotta, E.; Giordano, E.; Ferrante, A.; Clementi, F.; Lenci, S. Tracking Modal Parameter Evolution of Different Cultural Heritage Structure Damaged by Central Italy Earthquake of 2016. *Key Eng. Mater.* **2019**, *817*, 334–341. [CrossRef]
101. Pavlovic, M.; Trevisani, S.; Cecchi, A. A Procedure for the Structural Identification of Masonry Towers. *J. Nondestruct. Eval.* **2019**, *38*. [CrossRef]
102. Russo, G.; Bergamo, O.; Damiani, L.; Lugato, D. Experimental analysis of the "Saint Andrea" Masonry Bell Tower in Venice. A new method for the determination of "Tower Global Young's Modulus E". *Eng. Struct.* **2010**, *32*, 353–360. [CrossRef]
103. Bergamo, O.; Campione, G.; Russo, G. Testing of "Global Young's Modulus E" on a rehabilitated masonry bell tower in Venice. *Eng. Fail. Anal.* **2017**, *74*, 202–217. [CrossRef]
104. Rosa Valluzzi, M.; Da Porto, F.; Casarin, F.; Monteforte, N.; Modena, C. A contribution to the characterization of masonry typologies by using sonic waves investigations. *Actes J. Sci. LCPC* **2009**, *1*, 713–718.
105. Colapietro, D.; Fiore, A.; Netti, A.; Fatiguso, F.; Marano, G.; de Fino, M.; Cascella, D.; Ancona, A. Dynamic Identification and evaluation of the seismic safety of a masonry bell tower in the osuth of Italy. In Proceedings of the 4th International Conference on Computational Methods in Structural Dynamics and Earthquake Engineering (COMPDYN 2013), Athens, Greece, 12–14 June 2013. [CrossRef]

106. Bongiovanni, G.; Clemente, P.; Buffarini, G. Analysis of the seismic response of a damaged masonry bell tower. In Proceedings of the 12th World Conference on Earthquake Engineering, Auckland, New Zealand, 30 January–4 February 2000; Volume 30.
107. Ceriotti, M.; Mottola, L.; Picco, G.P.; Murphy, A.L.; Guna, S.; Corra, M.; Pozzi, M.; Zonta, D.; Zanon, P. Monitoring heritage buildings with wireless sensor networks: The Torre Aquila deployment. In Proceedings of the 2009 International Conference on Information Processing in Sensor Networks, San Francisco, CA, USA, 13–16 April 2009; pp. 277–288.
108. Sepe, V.; Speranza, E.; Viskovic, A. A method for large-scale vulnerability assessment of historic towers. *Struct. Control. Health Monit.* **2008**, *15*, 389–415. [CrossRef]
109. Ivorra, S.; Giannoccaro, N.I.; Foti, D. Simple model for predicting the vibration transmission of a squat masonry tower by base forced vibrations. *Struct. Control. Health Monit.* **2019**, *26*, e2360. [CrossRef]
110. Diaferio, M.; Foti, D.; Giannoccaro, N.I.; Ivorra, S. Identification of the modal properties of an historic masonry clock tower. In Proceedings of the SAHC2014—9th International Conference on Structural Analysis of Historical Constructions, Mexico City, Mexico, 14–17 October 2014; Volume 6.
111. Diaferio, M.; Foti, D.; Giannoccaro, N.; Vitti, M. On the use of modal analysis and ground penetrating radar test for the physical parameter identification of an historical bell tower. In Proceedings of the Vienna Congress on Recent Advances in Earthquake Engineering and structural Dynamics, Vienna, Austria, 28–30 August 2013; pp. 28–30.
112. Foti, D.; Diaferio, M.; Venerito, M. Non-Destructive Damage Detection and Retrofitting Techniques on a Historical Masonry Tower. In Proceedings of the 3rd International Balkans Conference on Challenges of Civil Engineering, Epoka, Albania, 19–21 May 2016.
113. Diaferio, M.; Foti, D. Seismic risk assessment of Trani's Cathedral bell tower in Apulia, Italy. *Int. J. Adv. Struct. Eng.* **2017**, *9*, 259–267. [CrossRef]
114. Pieraccini, M.; Dei, D.; Betti, M.; Bartoli, G.; Tucci, G.; Guardini, N. Dynamic identification of historic masonry towers through an expeditious and no-contact approach: Application to the "Torre del Mangia" in Siena (Italy). *J. Cult. Herit.* **2014**, *15*, 275–282. [CrossRef]
115. Pelella, T.; Mannara, G.; Cosenza, E.; Iervolino, I.; Lecce, L. Structural dynamic investigations on the bell tower from the S. Lucia's church–Serra S. Quirico, Ancona. In Proceedings of the 7th International Seminar on Seismic Isolation, Passive Energy Dissipation and Active Control of Vibrations of Structures, Assisi, Italy, 2–5 October 2001; pp. 2–5.
116. Cosenza, E.; Iervolino, I. Case Study: Seismic Retrofitting of a Medieval Bell Tower with FRP. *J. Compos. Constr.* **2007**, *11*, 319–327. [CrossRef]
117. Ferraioli, M.; Miccoli, L.; Abruzzese, D. Dynamic characterisation of a historic bell-tower using a sensitivity-based technique for model tuning. *J. Civ. Struct. Health Monit.* **2018**, *8*, 253–269. [CrossRef]
118. Beconcini, M.L.; Bennati, S.; Salvatore, W. Structural characterisation of a medieval bell tower: First historical, experimental and numerical investigations. *HIstor. Constr.* **2001**, 431–444.
119. Bennati, S.; Nardini, L.; Salvatore, W. Dynamic Behavior of a Medieval Masonry Bell Tower. II: Measurement and Modeling of the Tower Motion. *J. Struct. Eng.* **2005**, *131*, 1656–1664. [CrossRef]
120. Pieraccini, M. Extensive Measurement Campaign Using Interferometric Radar. *J. Perform. Constr. Facil.* **2017**, *31*. [CrossRef]
121. Bartoli, G.; Betti, M.; Giordano, S. In situ static and dynamic investigations on the "Torre Grossa" masonry tower. *Eng. Struct.* **2013**, *52*, 718–733. [CrossRef]
122. Zini, G.; Betti, M.; Bartoli, G.; Chiostrini, S. Frequency vs. time domain identification of heritage structures. *Procedia Struct. Integr.* **2018**, *11*, 460–469. [CrossRef]
123. Bassoli, E.; Vincenzi, L.; Altri, A.M.D.; de Miranda, S.; Forghieri, M.; Castellazzi, G. Ambient vibration-based finite element model updating of an earthquake-damaged masonry tower. *Struct. Control. Health Monit.* **2018**, *25*, e2150. [CrossRef]
124. Castellano, A.; Fraddosio, A.; Martorano, F.; Mininno, G.; Paparella, F.; Piccioni, M.D. Structural health monitoring of a historic masonry bell tower by radar interferometric measurements. In Proceedings of the 2018 IEEE Workshop on Environmental, Energy, and Structural Monitoring Systems (EESMS), Salerno, Italy, 21–21 June 2018. [CrossRef]
125. Clementi, F.; Ferrante, A.; Ribilotta, E.; Milani, G.; Lenci, S. *On the Dynamics of the Civic Clock Tower of Rotella (Ascoli Piceno) Severly Damaged by the Central Italy Seismic Sequence of 2016*; Pisa University Press: Pisa, Italy, 2019; pp. 81–89.
126. Abruzzese, D.; Vari, A. Vulnerabilità sismica di torri medievali in muratura. In Proceedings of the XI ANIDIS Conference, Genova, Italy, 25–29 June 2004.
127. Bonato, P.; Ceravolo, R.; Stephano, A.D.; Molinari, F. Cross-time frequency techniques for the identification of masonry buildings. *Mech. Syst. Signal Process.* **2000**, *14*, 91–109. [CrossRef]
128. Castagnetti, C.; Bassoli, E.; Vincenzi, L.; Mancini, F. Dynamic Assessment of Masonry Towers Based on Terrestrial Radar Interferometer and Accelerometers. *Sensors* **2019**, *19*, 1319. [CrossRef] [PubMed]
129. Vincenzi, L.; Bassoli, E.; Ponsi, F.; Castagnetti, C.; Mancini, F. Dynamic monitoring and evaluation of bell ringing effects for the structural assessment of a masonry bell tower. *J. Civ. Struct. Health Monit.* **2019**, *9*, 439–458. [CrossRef]
130. Pieraccini, M.; Parrini, F.; Dei, D.; Fratini, M.; Atzeni, C.; Spinelli, P. Dynamic characterization of a bell tower by interferometric sensor. *NDT&E Int.* **2007**, *40*, 390–396. [CrossRef]
131. Castellacci, I.; Spinelli, P.; Vignoli, A.; Galano, L. Caratterizzazione dinamica del campanile della pieve di San Cresci a Macioli nei pressi di Pratolino, comune di Vaglia, e progetto di miglioramento sismico. *Boll. Ing.* **2007**, *10*, 21–23.

132. Monchetti, S. On the Role of Uncertainties in the Seismic Risk Assessment of Historic Masonry Towers. Ph.D. Thesis, Technische Universität Braunschweig, Braunschweig, Germany, 2018.
133. Zonta, D.; Pozzi, M. The remarkable story of Portogruaro Civic Tower's probabilistic health monitoring. *Struct. Monit. Maint.* **2015**, *2*, 301–318. [CrossRef]
134. Lorenzoni, F.; Valluzzi, M.; Salvalaggio, M.; Minello, A.; Modena, C. Operational modal analysis for the characterization of ancient water towers in Pompeii. *Procedia Eng.* **2017**, *199*, 3374–3379. [CrossRef]
135. Atzeni, C.; Bicci, A.; Dei, D.; Fratini, M.; Pieraccini, M. Remote Survey of the Leaning Tower of Pisa by Interferometric Sensing. *IEEE Geosci. Remote Sens. Lett.* **2010**, *7*, 185–189. [CrossRef]
136. García-Macías, E.; Ierimonti, L.; Venanzi, I.; Ubertini, F. An Innovative Methodology for Online Surrogate-Based Model Updating of Historic Buildings Using Monitoring Data. *Int. J. Archit. Herit.* **2019**, *15*, 92–112. [CrossRef]
137. García-Macías, E.; Venanzi, I.; Ubertini, F. Metamodel-based pattern recognition approach for real-time identification of earthquake-induced damage in historic masonry structures. *Autom. Constr.* **2020**, *120*, 103389. [CrossRef]
138. García-Macías, E.; Kita, A.; Ubertini, F. Synergistic application of operational modal analysis and ambient noise deconvolution interferometry for structural and damage identification in historic masonry structures: Three case studies of Italian architectural heritage. *Struct. Health Monit.* **2019**, *19*, 1250–1272. [CrossRef]
139. García-Macías, E.; Ubertini, F. Automated operational modal analysis and ambient noise deconvolution interferometry for the full structural identification of historic towers: A case study of the Sciri Tower in Perugia, Italy. *Eng. Struct.* **2020**, *215*, 110615. [CrossRef]
140. Gentile, C.; Ruccolo, A.; Saisi, A. Long-Term Vibration Measurements to Enhance the Knowledge of a Historic Bell-Tower. In *RILEM Bookseries*; Springer International Publishing: Berlin/Heidelberg, Germany, 2019; pp. 2236–2244. [CrossRef]
141. Gentile, C.; Saisi, A. Ambient vibration testing of historic masonry towers for structural identification and damage assessment. *Constr. Build. Mater.* **2007**, *21*, 1311–1321. [CrossRef]
142. Ceroni, F.; Pecce, M.; Manfredi, G. Seismic Assessment of the Bell Tower of Santa Maria Del Carmine: Problems and Solutions. *J. Earthq. Eng.* **2009**, *14*, 30–56. [CrossRef]
143. Cavaleri, L.; Ferrotto, M.F.; Trapani, F.D.; Vicentini, A. Vibration Tests and Structural Identification of the Bell Tower of Palermo Cathedral. *Open Constr. Build. Technol. J.* **2019**, *13*, 319–330. [CrossRef]
144. Ubertini, F.; Comanducci, G.; Cavalagli, N.; Pisello, A.L.; Materazzi, A.L.; Cotana, F. Environmental effects on natural frequencies of the San Pietro bell tower in Perugia, Italy, and their removal for structural performance assessment. *Mech. Syst. Signal Process.* **2017**, *82*, 307–322. [CrossRef]
145. Tsogka, C.; Daskalakis, E.; Comanducci, G.; Ubertini, F. The Stretching Method for Vibration-Based Structural Health Monitoring of Civil Structures. *Comput.-Aided Civ. Infrastruct. Eng.* **2017**, *32*, 288–303. [CrossRef]
146. Hinzen, K.G.; Fleischer, C.; Schock-Werner, B.; Schweppe, G. Seismic Surveillance of Cologne Cathedral. *Seismol. Res. Lett.* **2012**, *83*, 9–22. [CrossRef]
147. Kuhlmann, W.; Butenweg, C.; López, M.; Fernández, S. Seismic Vulnerability Assessment of the Historic Aachen Cathedral Germany. In Proceedings of the 13th World Conference on Earthquake Engineering, Vancouver, BC, Canada, 1–6 August 2004.
148. Uglešić, D.; Uglešić, A. Case Studies of structural natural frequencies assessment and application in SHM and the calibration of FEM models. In Proceedings of the 1st Croatian Conference on Earthquake Engineering, Zagreb, Croatia, 22–24 March 2021. [CrossRef]
149. Gentile, C.; Canali, F. Continuous Monitoring the Cathedral of Milan: Design, Installation and Preliminary Results. In Proceedings of the the 18th International Conference on Experimental Mechanics, Brussels, Belgium, 1–5 June 2018. [CrossRef]
150. Busca, G.; Cappellini, A.; Cigada, A.; Vanali, M. Operational modal Analysis of the "Guglia Maggiore" of the "Duomo" in Milano. In Proceedings of the 4th International Operational Modal Analysis Conference IOMAC 2011, Istanbul, Turkey, 9–11 May 2011; pp. 1–8.
151. Wilson, J.M.; Selby, A.R. Durham Cathedral tower vibrations during bell-ringing. In *Engineering a Cathedral*; Thomas Telford Publishing: London, UK, 1993; pp. 77–100. [CrossRef]
152. Rebelo, C.; Júlio, E.; Costa, D. Modal identification of the Coimbra University tower. In Proceedings of the 2nd International Operational Modal Analysis Conference, Copenhagen, Denmark, 30 April–2 May 2007; pp. 177–184.
153. Foti, D.; Diaferio, M.; Giannoccaro, N.I.; Mongelli, M. Ambient vibration testing, dynamic identification and model updating of a historic tower. *NDT&E Int.* **2012**, *47*, 88–95. [CrossRef]
154. Garcia Garcia, I.; Pardo, A; Pelayo, F.; Martin A.; Aenlle Lopez, M. Modal analysis of the tower of the Laboral City of Culture (Conference Paper). In Proceedings of the 6th International Operational Modal Analysis Conference, Gijon, Spain, 12–14 May 2015.
155. Rainieri, C.; Gargaro, D.; Fabbrocino, G. The role of operational modal analysis in the non-destructive assessment of an Italian Monument. In Proceedings of the 6th International Operational Modal Analysis Conference, Gijon, Spain, 12–14 May 2015.
156. Jardim, C.M.; Mendes, L.A.; Gonçalve, A.M. Dynamic characterization of the Funchal's cathedral bell tower. In Proceedings of the 5th International Operational Modal Analysis Conference, Guimaraes, Portugal, 13–15 May 2013.
157. Salachoris, G.P.; Standoli, G.; Betti, M.; Milani, G.; Clementi, F. Evolutionary numerical model for cultural heritage structures via genetic algorithms: A case study in central Italy. *Bull. Earthq. Eng.* **2023**. [CrossRef]

158. Patron-Solares, A.; Cremona, C.; Bottineau, C.; Leconte, R.; Goepfer, F. Study of bell swinging induced vibrations of bell tower of Metz cathedral (France). *Actes J. Sci. LCPC* **2005**, *1*, 529–536.
159. Ditommaso, R.; Mucciarelli, M.; Parolai, S.; Picozzi, M. Monitoring the structural dynamic response of a masonry tower: Comparing classical and time-frequency analyses. *Bull. Earthq. Eng.* **2012**, *10*, 1221–1235. [CrossRef]
160. Kolaj, M.; Adams, J. Dynamic characteristics of Canada's Parliament Hill towers from ambient vibrations and recorded earthquake data. *Can. J. Civ. Eng.* **2021**, *48*, 16–25. [CrossRef]
161. Peña, F.; Manzano, J. Dynamical Characterization of Typical Mexican Colonial Churches. In *Computational Methods in Applied Sciences*; Springer International Publishing: Berlin/Heidelberg, Germany, 2015; pp. 297–319. [CrossRef]
162. Manos, G.; Kozikopoulos, E. In-situ measured dynamic response of the bell tower of Agios Gerasimos in Lixouri Kefalonia, Greece and its utilization in the numerical predictions of its earthquake response. In Proceedings of the 5th International Conference on Computational Methods in Structural Dynamics and Earthquake Engineering (COMPDYN 2015), Athens, Greece, 25–27 May 2015. [CrossRef]
163. Ubertini, F.; Comanducci, G.; Cavalagli, N. Vibration-based structural health monitoring of a historic bell-tower using output-only measurements and multivariate statistical analysis. *Struct. Health Monit.* **2016**, *15*, 438–457. [CrossRef]
164. Ribilotta, E.; Clementi, F.; Pellegrino, M.; Poiani, M.; Gazzani, V.; Santilli, G.; Lenci, S. Monitoring cultural heritage buildings: The San Ciriaco bell-tower in Ancona. *AIP Conf. Proc.* **2018**, *2040*, 090005 . [CrossRef]
165. Baraccani, S.; Azzara, R.M.; Palermo, M.; Gasparini, G.; Trombetti, T. Long-Term Seismometric Monitoring of the Two Towers of Bologna (Italy): Modal Frequencies Identification and Effects Due to Traffic Induced Vibrations. *Front. Built Environ.* **2020**, *6*, 85. [CrossRef]
166. Sánchez-Aparicio, L.J.; Riveiro, B.; González-Aguilera, D.; Ramos, L.F. The combination of geomatic approaches and operational modal analysis to improve calibration of finite element models: A case of study in Saint Torcato Church (Guimarães, Portugal). *Constr. Build. Mater.* **2014**, *70*, 118–129. [CrossRef]
167. Scamardo, M.; Zucca, M.; Crespi, P.; Longarini, N.; Cattaneo, S. Seismic Vulnerability Evaluation of a Historical Masonry Tower: Comparison between Different Approaches. *Appl. Sci.* **2022**, *12*, 11254. [CrossRef]
168. Casarin, F.; Modena, C. Seismic Assessment of Complex Historical Buildings: Application to Reggio Emilia Cathedral, Italy. *Int. J. Archit. Herit.* **2008**, *2*, 304–327. [CrossRef]
169. Spinelli, P.; Salvatori, L.; Lancellotta, R.; Betti, M. Preliminary Assessment Of The Seismic Behaviour Of Giotto's Bell Tower In Florence. *Int. J. Archit. Herit.* **2022**, *17*, 23–45. [CrossRef]
170. Ramírez, E.; Lourenço, P.B.; D'Amato, M. Seismic Assessment of the Matera Cathedral. In *RILEM Bookseries*; Springer International Publishing: Berlin/Heidelberg, Germany, 2019; pp. 1346–1354. [CrossRef]
171. Mendes, P.; Baptista, M.; Agostinho, L.; Lagomarsino, S.; Costav, J. Structural and dynamic analysis of N. Sra. do Carmo church, Lagos Portugal. In Proceedings of the EURODYN 2005, Structural Dynamics, Paris, France, 4–7 September 2005; pp. 311–318.
172. Baptista, M.; Mendes, P.; Afilhado, A.; Agostinho, L.; Lagomarsino, A.; Victor, L.M. Ambient vibration testing at N. Sra. do Carmo Church, preliminary results. In Proceedings of the 4th International Seminar on Structural analysis of Historical Constructions, Bath, UK, 2–4 July 2004; pp. 483–488.
173. Ramos, L.F.; Aguilar, R.; Lourenço, P.B.; Moreira, S. Dynamic structural health monitoring of Saint Torcato church. *Mech. Syst. Signal Process.* **2013**, *35*, 1–15. [CrossRef]
174. Aguilar, R.; Noel, M.F.; Ramos, L.F. Integration of reverse engineering and non-linear numerical analysis for the seismic assessment of historical adobe buildings. *Autom. Constr.* **2019**, *98*, 1–15. [CrossRef]
175. Ivancic, S.R.; Briceno, C.; Marques, R.; Aguilar, R.; Perucchio, R.; Vargas, J. Seismic assessment of the St. Peter apostle church of Andahuaylillas in Cusco, Peru. In Proceedings of the SAHC2014–9th International Conference on Structural Analysis of Historical Constructions, Mexico City, Mexico, 14–17 October 2014.
176. Zonno, G.; Aguilar, R.; Castañeda, B.; Boroschek, R.; Lourenço, P.B. Environmental and Dynamic Remote Monitoring of Historical Adobe Buildings: The Case Study of the Andahuaylillas Church in Cusco, Peru. In *RILEM Bookseries*; Springer International Publishing: Berlin/Heidelberg, Germany, 2019; pp. 2216–2224. [CrossRef]
177. Peña, F.; Lourenço, P.B.; Mendes, N. Seismic assessment of the Qutb minar in Delhi, India. In Proceedings of the 14th World Conference on Earthquake Engineering, Beijing, China, 12–17 October 2008; pp. 483–488.
178. Masciotta, M.G.; Ramos, L.F. Dynamic identification of historic masonry structures. In *Long-Term Performance and Durability of Masonry Structures*; Elsevier: Amsterdam, The Netherlands, 2019; pp. 241–264.
179. Pineda, P.; Sáez, A. Assessment of ancient masonry slender towers under seismic loading: Dynamic characterization of the Cuatrovitas tower. In *Heritage Masonry*; WIT Press: Billerica, MA, USA, 2013; pp. 143–157. [CrossRef]
180. Buachart, C.; Hansapinyo, C.; Tantisukhuman, N.; Miyamoto, M.; Matsushima, M.; Limkatanyu, S.; Imjai, T.; Zhang, H. Real time vibration measurement and inverse analysis for dynamic properties of an axisymmetric masonry structure. *J. Asian Archit. Build. Eng.* **2022**, 1–10. [CrossRef]
181. Francisca, S.L. Dynamic Characterisation of the Bell Tower of Sant Cugat Monastery. Master's Thesis, Universitat Politècnica de Catalunya, Barcelona, Spain, 2020.
182. Italian Ministry of Infrastructure. *Norme Tecniche per le Costruzioni—DM 14 Gennaio 2008*; Supplemento Ordinario; Italian Ministry of Infrastructure: Rome, Italy, 2008.

183. Rodrigues, J.M.V.B.L. *Identificação modal estocástica: Métodos de análise e aplicações em estruturas de engenharia civil*; FEUP: Porto, Portugal, 2005.
184. Cantieni, R. Experimental methods used in system identification of civil engineering structures. In Proceedings of the International Operational Modal Analysis Conference (IOMAC), Copenhagen, Denmark, 26–27 April 2005; pp. 249–260.
185. Masjedian, M.; Keshmiri, M. A review on operational modal analysis researches: Classification of methods and applications. In Proceedings of the 3rd IOMAC, Portonovo, Italy, 4–6 May 2009; pp. 707–718.
186. Zhang, L.; Wang, T.; Tamura, Y. A frequency–spatial domain decomposition (FSDD) method for operational modal analysis. *Mech. Syst. Signal Process.* **2010**, *24*, 1227–1239. [CrossRef]
187. Brincker, R.; Zhang, L.; Andersen, P. Modal identification from ambient responses using frequency domain decomposition. In Proceedings of the 18th international Modal Analysis Conference (IMAC), San Antonio, TX, USA, 7–10 February 2000; Volume 1, pp. 625–630.
188. Overchee, P.; Moor, B. *Subspace Identification for Linear System*; Atlantis Press: Amsterdam, The Netherlands, 1996.
189. Casolo, S.; Diana, V.; Uva, G. Influence of soil deformability on the seismic response of a masonry tower. *Bull. Earthq. Eng.* **2017**, *15*, 1991–2014. [CrossRef]
190. de Silva, F.; Pitilakis, D.; Ceroni, F.; Sica, S.; Silvestri, F. Experimental and numerical dynamic identification of a historic masonry bell tower accounting for different types of interaction. *Soil Dyn. Earthq. Eng.* **2018**, *109*, 235–250. [CrossRef]
191. Traill-Nash, R.; Collar, A. The effects of shear flexibility and rotatory inertia on the bending vibrations of beams. *Q. J. Mech. Appl. Math.* **1953**, *6*, 186–222. [CrossRef]
192. Nallim, L.G.; Grossi, R.O. A general algorithm for the study of the dynamical behaviour of beams. *Appl. Acoust.* **1999**, *57*, 345–356. [CrossRef]
193. Cowper, G. The shear coefficient in Timoshenko's beam theory. *J. Appl. Mech.* **1966**, *33*, 335–340. [CrossRef]
194. Meirovitch, L. *Analytical Methods in Vibrations*; McMillan: New York, NY, USA, 1967.
195. Mazanoglu, K. Natural frequency analyses of segmented Timoshenko–Euler beams using the Rayleigh–Ritz method. *J. Vib. Control.* **2017**, *23*, 2135–2154. [CrossRef]
196. Combescure, A.; Hoffmann, A.; Pasquet, P. The CASTEM finite element system. In *Finite Element Systems: A Handbook*; Springer: Berlin/Heidelberg, Germany, 1982; pp. 115–125.
197. Gatelli, D.; Kucherenko, S.; Ratto, M.; Tarantola, S. Calculating first-order sensitivity measures: A benchmark of some recent methodologies. *Reliab. Eng. Syst. Saf.* **2009**, *94*, 1212–1219. [CrossRef]
198. Saltelli, A.; Tarantola, S.; Chan, K.S. A quantitative model-independent method for global sensitivity analysis of model output. *Technometrics* **1999**, *41*, 39–56. [CrossRef]
199. Cukier, R.; Fortuin, C.; Shuler, K.E.; Petschek, A.; Schaibly, J.H. Study of the sensitivity of coupled reaction systems to uncertainties in rate coefficients. I Theory. *J. Chem. Phys.* **1973**, *59*, 3873–3878. [CrossRef]
200. Tarantola, S.; Gatelli, D.; Mara, T.A. Random balance designs for the estimation of first order global sensitivity indices. *Reliab. Eng. Syst. Saf.* **2006**, *91*, 717–727. [CrossRef]
201. Mara, T.A. Extension of the RBD-FAST method to the computation of global sensitivity indices. *Reliab. Eng. Syst. Saf.* **2009**, *94*, 1274–1281. [CrossRef]
202. Jacques, J. *Contributions to Sensitivity Analysis and Generalized Discriminant Analysis*; Technical Report; University Joseph Fourier: Grenoble, France, 2005.
203. Helton, J.C.; Johnson, J.D.; Sallaberry, C.J.; Storlie, C.B. Survey of sampling-based methods for uncertainty and sensitivity analysis. *Reliab. Eng. Syst. Saf.* **2006**, *91*, 1175–1209. [CrossRef]
204. Xu, C.; Gertner, G.Z. Uncertainty and sensitivity analysis for models with correlated parameters. *Reliab. Eng. Syst. Saf.* **2008**, *93*, 1563–1573. [CrossRef]
205. Fernandes, V.A.; Lopez-Caballero, F.; d'Aguiar, S.C. Probabilistic analysis of numerical simulated railway track global stiffness. *Comput. Geotech.* **2014**, *55*, 267–276. [CrossRef]
206. Gaspar, A.; Lopez-Caballero, F.; Modaressi-Farahmand-Razavi, A.; Gomes-Correia, A. Methodology for a probabilistic analysis of an RCC gravity dam construction. Modelling of temperature, hydration degree and ageing degree fields. *Eng. Struct.* **2014**, *65*, 99–110. [CrossRef]
207. Sobol, I.M. Global sensitivity indices for nonlinear mathematical models and their Monte Carlo estimates. *Math. Comput. Simul.* **2001**, *55*, 271–280. [CrossRef]
208. Herman, J.; Usher, W. SALib: An open-source Python library for sensitivity analysis. *J. Open Source Softw.* **2017**, *2*, 97. [CrossRef]